

1 **Halocarbon emissions and sources in the equatorial**
2 **Atlantic Cold Tongue**

3
4 **Helmke Hepach¹, Birgit Quack¹, Stefan Raimund¹, Tim Fischer¹, Elliot L. Atlas²,**
5 **and Astrid Bracher^{3,4}**

6 [1]GEOMAR Helmholtz Centre for Ocean Research Kiel, Germany

7 [2]Rosenstiel School of Marine and Atmospheric Science (RSMAS), University of Miami,
8 USA

9 [3]Helmholtz-University Young Investigators Group PHYTOOPTICS, Alfred-Wegener-
10 Institute (AWI) Helmholtz Center for Polar and Marine Research, Bremerhaven

11 [4]Institute of Environmental Physics, University of Bremen, Germany

12
13 Corresponding author: H. Hepach, GEOMAR Helmholtz Centre for Ocean Research Kiel,
14 Germany, Research Division 2: Marine Biogeochemistry, Chemical Oceanography
15 Düsternbrooker Weg 20, 24105 Kiel, Germany (hhepach@geomar.de)

1 **Abstract**

2 Halocarbons from oceanic sources contribute to halogens in the troposphere, and can be
3 transported into the stratosphere where they take part in ozone depletion. This paper presents
4 distribution and sources in the equatorial Atlantic from June and July 2011 of the four
5 compounds bromoform (CHBr_3), dibromomethane (CH_2Br_2), methyl iodide (CH_3I) and
6 diiodomethane (CH_2I_2). Enhanced biological production during the Atlantic Cold Tongue
7 (ACT) season, indicated by phytoplankton pigment concentrations, led to elevated
8 concentrations of CHBr_3 of up to 44.7 pmol L^{-1} and up to 9.2 pmol L^{-1} for CH_2Br_2 in surface
9 water, which is comparable to other tropical upwelling systems. While both compounds
10 correlated very well with each other in the surface water, CH_2Br_2 was often more elevated in
11 greater depth than CHBr_3 , which showed maxima in the vicinity of the deep chlorophyll
12 maximum. The deeper maximum of CH_2Br_2 indicates an additional source in comparison to
13 CHBr_3 or a slower degradation of CH_2Br_2 . Concentrations of CH_3I of up to 12.8 pmol L^{-1} in
14 the surface water were measured. In contrary to expectations of a predominantly
15 photochemical source in the tropical ocean, its distribution was mostly in agreement with
16 biological parameters, indicating a biological source. CH_2I_2 was very low in the near surface
17 water with maximum concentrations of only 3.7 pmol L^{-1} . CH_2I_2 showed distinct maxima in
18 deeper waters similar to CH_2Br_2 . For the first time, diapycnal fluxes of the four halocarbons
19 from the upper thermocline into and out of the mixed layer were determined. These fluxes
20 were low in comparison to the halocarbon sea-to-air fluxes. This indicates that despite the
21 observed maximum concentrations at depth, production in the surface mixed layer is the main
22 oceanic source for all four compounds and one of the main driving factors of their emissions
23 into the atmosphere in the ACT-region. The calculated production rates of the compounds in
24 the mixed layer are $34 \pm 65 \text{ pmol m}^{-3} \text{ h}^{-1}$ for CHBr_3 , $10 \pm 12 \text{ pmol m}^{-3} \text{ h}^{-1}$ for CH_2Br_2 , 21 ± 24
25 $\text{pmol m}^{-3} \text{ h}^{-1}$ for CH_3I and $384 \pm 318 \text{ pmol m}^{-3} \text{ h}^{-1}$ for CH_2I_2 determined from 13 depth
26 profiles.

27

28 **1 Introduction**

29 Oceanic upwelling regions where cold nutrient rich water is brought to the surface are
30 connected to enhanced primary production and elevated halocarbon production, especially of
31 bromoform (CHBr_3) and dibromomethane (CH_2Br_2) (Quack et al., 2007a; Carpenter et al.,
32 2009; Raimund et al., 2011; Hepach et al., 2014). Photochemical formation (Moore and
33 Zafiriou, 1994; Richter and Wallace, 2004) with a possible involvement of organic precursors
34 is an important source for methyl iodide (CH_3I). An abiotic formation pathway for

1 halocarbons involving ozone has been found for diiodomethane (CH_2I_2) in the laboratory
2 (Martino et al., 2009). But, its production is generally suggested to be biotic, occurring likely
3 through different species of phytoplankton than are involved in the production of CHBr_3 and
4 CH_2Br_2 (Moore et al., 1996; Orlikowska and Schulz-Bull, 2009). Additionally, bacterial
5 involvement in the formation of halocarbons e.g. CH_3I and CH_2I_2 has been observed in the
6 field and the laboratory (Manley and Dastoor, 1988; Amachi et al., 2001; Fuse et al., 2003;
7 Amachi, 2008). Large uncertainties regarding the production of halocarbons in the ocean
8 remain. Depth profiles of the different compounds provide insight into the processes
9 participating in their cycling. Elevated concentrations of CHBr_3 and CH_2Br_2 at the bottom of
10 the mixed layer and below, often close to the chlorophyll *a* (Chl *a*) subsurface maximum, are
11 a common feature in the water column (Yamamoto et al., 2001; Quack et al., 2004; Liu et al.,
12 2013a), and are attributed to enhanced production by phytoplankton. While occasionally CH_3I
13 maxima close to the Chl *a* maximum were observed as well (Moore and Groszko, 1999;
14 Wang et al., 2009), Happell and Wallace (1996) ascribed surface maxima in several oceanic
15 regions including the equatorial Atlantic to a predominantly photochemical source. Rapid
16 photolysis and biogenic sources in the deep Chl *a* maximum are suggested to determine the
17 depth distribution of CH_2I_2 concentrations (Moore and Tokarczyk, 1993; Yamamoto et al.,
18 2001; Carpenter et al., 2007; Kurihara et al., 2010). The complex interactions between the
19 sources (biogenic and non-biogenic production), sinks (hydrolysis, photolysis, chlorine
20 substitution and air-sea gas exchange), advection, and turbulent mixing in and out of the
21 mixed layer (diapycnal fluxes), which determine the water concentrations of these
22 compounds, are still sparsely investigated.

23 Once they are produced in the ocean, halocarbons can be transported from the oceanic mixed
24 layer into the troposphere via air-sea gas transfer. CHBr_3 and CH_2Br_2 are the largest
25 contributors to atmospheric organic bromine from the ocean (Penkett et al., 1985; Schauffler
26 et al., 1998; Hossaini et al., 2012). Marine CH_3I is the most abundant organoiodine in the
27 troposphere, while the very short lived CH_2I_2 and CH_2ClI contribute potentially as much
28 organic iodine (Saiz-Lopez et al., 2012). Significant amounts of halocarbons and their
29 degradation products can be carried into the stratosphere (Solomon et al., 1994; Hossaini et
30 al., 2010; Aschmann et al., 2011), especially in the tropical regions where surface air can be
31 transported very rapidly into the tropical tropopause layer by tropical deep convection
32 (Tegtmeier et al., 2012; Tegtmeier et al., 2013). The short-lived brominated and iodinated
33 halocarbons produced in the equatorial region may hence play an important role for
34 stratospheric halogens.

1 This paper characterizes the distribution of CHBr_3 , CH_2Br_2 , CH_3I , and CH_2I_2 in the surface
2 water and the water column of the equatorial Atlantic Cold Tongue (ACT) for the first time.
3 The ACT is a known feature in the equatorial region, which is characterized by intensive
4 cooling of SSTs. This cooling is also associated with phytoplankton blooms (Grotsky et al.,
5 2008) as potential source for halocarbons. CHBr_3 , CH_2Br_2 , CH_3I and CH_2I_2 represent the most
6 important carriers of organic halogens into the troposphere, which have important
7 implications for atmospheric chemistry and are poorly characterized in the ACT region. We
8 therefore aim to provide more insight into the biological and physical processes contributing
9 to the mixed layer budget of halocarbons in the equatorial Atlantic. Sea-to-air fluxes and, for
10 the first time, diapycnal fluxes from the upper thermocline are calculated as sources and sinks
11 for the mixed layer. Phytoplankton groups (obtained from pigment concentrations) are
12 evaluated as potential sources of these four compounds. Additionally, surface water
13 halocarbons are correlated to meta data such as temperature, salinity and global radiation to
14 understand their distribution further. Finally, we estimate production rates for the mixed layer
15 of the ACT region.

16

17 **2 Methods**

18 Cruise MSM18/3 onboard the RV *Maria S. Merian* took place from June 21 to July 21 2011.
19 One goal of the campaign was the characterization of the Atlantic equatorial upwelling with
20 regard to halocarbon emissions and their sources. RV *Maria S. Merian* started in Mindelo
21 (Sao Vicente, Cape Verde) at 16.9°N and 25.0°W , and finished in Libreville (Gabon) at
22 0.4°N and 13.4°E with several transects across the equator. The ship entered the ACT
23 several times. Measurements of halocarbons and phytoplankton pigments were conducted in
24 surface water along the cruise track, and at 13 stations (Figure 1). Samples for dissolved
25 halocarbons from sea surface water were taken from a continuously working pump in the
26 ships moon pool at a depth of about 6.5 m every 3 h. Deep water samples were taken from up
27 to eight different depths per station between 10 and 700 m from 12 L Niskin bottles attached
28 to a 24-bottle-rosette with a CTD (Conductivity Temperature Depth). Halocarbon stations 1 –
29 4 were located at the first meridional transect across the ACT at 15°W , stations 5 – 7 at the
30 second transect at 10°W , 8 – 10 were located at the third section at around 5°W , and the last
31 three stations 11 – 13 were taken during the last section at 0°E (Figure 1). Water temperature
32 and salinity were recorded with a thermosalinograph. Air pressure and wind speed were
33 derived from sensors in 30 m height, averaged in 10 min intervals, and wind speed was
34 corrected to 10 m. Global radiation was measured onboard in 19.5 m height with sensors

1 (SMS-1 combined system from MesSen Nord, Germany) measuring downward incoming
2 global radiation (GS, shortwave) and infrared radiation (IR, long-wave).

3 **2.1 Sampling and analysis of halocarbons in seawater**

4 A purge and trap system attached to a gas chromatograph with mass spectrometric detection
5 (GC-MS) in single ion mode was used to analyze 50 mL water samples for dissolved
6 halocarbons. Volumetrically prepared standards in methanol were used for quantification.
7 Precision lay within 3 % for CHBr_3 , 6 % for CH_2Br_2 , 15 % for CH_3I and 20 % for CH_2I_2
8 determined from duplicates. For a detailed description see Hepach et al. (2014).

9 **2.2 Phytoplankton pigment analysis and continuous measurement of** 10 **chlorophyll a**

11 Water samples were filtered onto GF/F filters, shock-frozen in liquid nitrogen and stored
12 at -80°C . Pigments listed in Table 1 of Taylor et al. (2011) were analyzed using a HPLC
13 technique according to Barlow et al. (1997) as described in Taylor et al. (2011). Surface
14 pigment data were already used in a study by Bracher et al. (2015). All pigment data are
15 already published and available from PANGAEA
16 (<http://doi.pangaea.de/10.1594/PANGAEA.848586>). For interpretation of the pigment data,
17 CHEMTAX® (Mackey et al., 1996) was used, and initiated with the pigment ratio matrix
18 proposed by Veldhuis and Kraay (2004) for the subtropical Atlantic Ocean. The following
19 phytoplankton groups were evaluated: *diatoms*, *Synechococcus*-type, *Prochlorococcus* HL
20 (high light adapted) and *Prochlorococcus* LL (low light adapted), *dinoflagellates*,
21 *haptophytes*, *pelagophytes*, *cryptophytes* and *prasinophytes*.

22 10-min-averaged continuous surface maximum fluorescence measured by a microFlu-chl
23 fluorometer from TriOS located in the ships moon pool was used to derive continuous total
24 Chl *a* (TChl *a*) concentrations along the underway transect. This is based on the assumption
25 that active fluorescence *F* is correlated to the amount of available TChl *a* (Kolber and
26 Falkowski, 1993). The method to convert fluorescence to TChl *a* is described in detail in
27 Taylor et al. (2011). Mean conversion factors specific for each zone were determined for
28 collocated *F* and HPLC-TChl *a* (the sum of monovinyl Chl *a*, divinyl Chl *a* and
29 Chlorophyllide *a*; the latter is mainly formed as artefact of the former two during the
30 extraction process and therefore included in the calculation) measurements. A linear
31 regression of $r = 0.83$ ($p < 0.01$, $n = 89$) was observed between surface HPLC-derived TChl *a*
32 and *F*-derived TChl *a*, which indicates the robustness of the conversion of *F* to TChl *a*. The
33 high depth resolved chlorophyll profiles were derived from fluorescence values obtained from

1 a Dr. Haardt fluoremeter mounted to the CTD and calibrated with collocated HPLC-derived
2 TChl *a* concentrations at six depths of each profile according to Fujiki et al. (2011).

3 **2.3 Correlation analysis of halocarbons**

4 Different parameters were correlated to surface water halocarbons. Physical influences were
5 investigated with 10 min averages of sea surface temperature (SST), sea surface salinity
6 (SSS), global radiation and wind speed, and a relationship with location was explored using
7 latitude. Biological parameters used for correlations were TChl *a*, and the abundances of all
8 phytoplankton groups. Since most of the data sets were not normally distributed and common
9 transformations into normal distributions were not possible, the Spearman's rank correlation
10 coefficient r_s was applied. All correlations with $p < 0.05$ were regarded as significant.

11 Correlation analysis of the entire depth profile dataset using the Spearman's rank coefficient
12 did not allow for drawing specific conclusions due to the complexity of the data set. Hence,
13 the mixed influences on water column halocarbon concentrations were examined with
14 principal component analysis (PCA) using MATLAB®. PCA analyzes the collective variance
15 of a dataset including several variables. The PCA has the advantage to simplify a complex
16 data set and find similarities. Concentrations of all four halocarbons, all phytoplankton
17 groups, the TChl *a*, density, temperature, and salinity were included.

18 **2.4 Mixed layer depth**

19 Mixed layer depths z_{ML} were determined using the method introduced by Kara et al. (2000). It
20 proved to be closest to the visually determined z_{ML} from the temperature, salinity and density
21 profiles. The mixed layer of each CTD profile was calculated as the depth where the
22 temperature from the reference depth in the upper well-mixed temperature region was reduced
23 by a threshold value of 0.8 °C.

24 **2.5 Calculation of sea-to-air fluxes of halocarbons**

25 The air-sea gas exchange parameterization of Nightingale et al. (2000) was applied to
26 calculate sea-to-air fluxes F_{as} of halocarbons (equation 1). Schmidt number corrections as
27 reported by Quack and Wallace (2003) were applied to determine the compound specific
28 transfer coefficient k_w . The air-sea concentration gradient was computed from sea surface
29 water measurements and mean atmospheric mixing ratios c_{atm} of 2.50 ppt for CHBr₃, 1.20 ppt
30 for CH₂Br₂, and 0.50 ppt for CH₃I determined from 10 atmospheric data points during
31 MSM18/3, and atmospheric mixing ratios of 0.01 ppt for CH₂I₂ as reported by Jones et al.
32 (2010) for the tropical Atlantic. Henry's law constants H of Moore and co-workers (Moore et
33 al., 1995a; Moore et al., 1995b) were used to obtain the equilibrium concentrations c_{atm}/H .

$$F_{as} = k_w \cdot \left(c_w - \frac{c_{atm}}{H} \right) \quad (1)$$

2.6 Calculation of diapycnal fluxes of halocarbons

To estimate the halocarbon transport perpendicular to the stratification, equation 2 was used with F_{dia} as the diapycnal flux in $\text{mol m}^{-2} \text{s}^{-1}$, ρ as the seawater density in kg m^{-3} , Δc being the diapycnal gradient of the concentration in mol kg^{-1} , and K_{dia} as the diapycnal diffusion coefficient in $\text{m}^2 \text{s}^{-1}$.

$$F_{dia} = \rho \cdot K_{dia} \cdot \Delta c \quad (2)$$

In the equatorial near surface water, molecular and double diffusion are negligible compared to turbulent mixing. K_{dia} from turbulent mixing can be estimated from measurements of the velocity microstructure (turbulent motions on length scales of centimeters to meters). During MSM18/3, velocity microstructure profiling was performed immediately before or after taking halocarbon profiles, so that local and pointwise in time estimates of the diapycnal flux resulted from the combination of the two profiles via equation 2. The microstructure profiler (MSS) was a loosely tethered MSS90 equipped with airfoil shear probes, manufactured by Sea & Sun Technology. In order to calculate K_{dia} from velocity fluctuations measured by the MSS, first the average spectrum of vertical shear for a depth interval of typically 10 to 50 m was calculated and integrated to get an estimate of the average dissipation rate of turbulent kinetic energy (epsilon in W kg^{-1}). Equation 3, first proposed by Osborn (1980) allows to deduce K_{dia} , with γ a function of the mixing efficiency and N the buoyancy frequency for the chosen depth interval.

$$K_{dia} = \gamma \cdot \frac{\epsilon}{N^2} \quad (3)$$

γ was chosen to be 0.2 following Hummels et al. (2013) for the tropical Atlantic. A more detailed description of the method to derive K_{dia} and diapycnal fluxes below the mixed layer can be found in Schafstall et al. (2010), Hummels et al. (2013), and Schlundt et al. (2014).

25

3 Physical and biological characteristics of the investigation area

3.1 Oceanographic description

The equatorial Atlantic is described by a complex current system. The surface is characterized by the westward South Equatorial Current (SEC), which spreads between 3°N and 15°S and reaches as deep as 100 m, but has shallow mixed layers close to the equator (Tomczak and

1 Godfrey, 2005). The Equatorial Undercurrent (EUC) can be found below the SEC (Molinari,
2 1982), and is a narrow band between 2° N and 2° S flowing towards the east while reducing
3 speed. It carries mostly water with characteristics of deeper tropical surface water (TSW) and
4 of shallower central water. TSW around and north of the equator is characterized by high
5 temperatures and comparably low salinities due to enhanced precipitation (Tsuchiya et al.,
6 1992). While the core of the EUC in the west is at 100 m, its position in the east follows the
7 seasonal vertical migration of the thermocline (Stramma and Schott, 1999). In agreement with
8 this, the mixed layer depth was shallow and ranged only between surface and 49 m with a
9 mean of 28 m during MSM18/3. The mixed layer was also exposed to diurnal variability.
10 During daytime, it was shallower due to warmer air temperatures and more stratification. At
11 night, when the air temperature and SSTs cool, water mixes further down. The shallowest
12 mixed layers were found between 0° N and 3° S in agreement with the location of the EUC.
13 The Atlantic Cold Tongue (ACT) is a known feature in the equatorial region where SSTs
14 between 20° and 5° W can drop by 5 – 7 °C during May to September (Weingartner and
15 Weisberg, 1991). Many uncertainties remain with respect to the exact mechanisms that lead to
16 the development of the ACT. Jouanno et al. (2011) suggested that the strong increase of the
17 westward SEC associated with the ITCZ (Philander and Pacanowski, 1986), and the
18 maximum shear above the core of the underlying EUC lead to the low SSTs, confirmed later
19 by microstructure measurements (Hummels et al., 2013; Schlundt et al., 2014). Although the
20 shear is maximal at 0° E, maximum cooling appears at 10° W due to the stronger stratification
21 in the eastern basin of the equatorial Atlantic. SSTs during MSM18/3 of mean (range) 24.4
22 (22.1 – 29.0) °C and SSSs of 35.7 (34.5 – 36.3) were measured in the investigated region
23 (Table 1, Figure 2). Generally, high SSTs and low SSSs of less than 35.5 in the TSW were
24 observed north of the equator. Lower SSTs and higher SSSs were measured in the South
25 except for the 10° W section where these low SSTs and high SSSs were also found north of
26 the equator. Maximum SSTs around the equator of 28.5 °C were found at 3° N and 20° W,
27 while the lowest SSTs of 22.1 °C were located at 1° N and 10° W (Figure 1, Figure 2, Table
28 1).

29 **3.2 Biological description**

30 The cooling of SSTs in the ACT region is usually accompanied by a phytoplankton bloom.
31 Grodsky et al. (2008) found a seasonal peak of TChl *a* of 0.60 µg L⁻¹ in boreal summer. In
32 comparison, surface TChl *a* during MSM18/3 reached values as high as 1.20 µg L⁻¹ around
33 0.8° N and 0° E (Figure 2c). Very high TChl *a* concentrations above 1.00 µg L⁻¹ were also
34 measured from the continuous fluorescence sensor around 10° W, coincidentally with the

1 most intense cooling. The three hourly HPLC measurements of up to $0.99 \mu\text{g L}^{-1}$ generally
2 also agree with the high TChl *a* maximum values measured with the fluorescence sensor (Fig.
3 2, Table 1). Additionally, nitrate and phosphate were significantly anticorrelated with SST
4 (not shown), hence the upwelled water of the EUC was connected to enhanced biological
5 production.

6 The most abundant phytoplankton group in the ACT were *chrysophytes* in both surface water
7 and depth profiles during MSM18/3 (Figure 2a). *Chrysophytes*, golden algae with flagellar
8 hairs, are thought to be mostly common in freshwater (Round, 1986). Nevertheless, they have
9 been previously shown to be also the most abundant phytoplankton group in several regions
10 of the Atlantic ocean, including the lower latitudes around the equator (Kirkham et al., 2011).
11 This group correlated significantly with SST ($r_s = -0.45$) and SSS ($r_s = 0.48$) (Table 2), it
12 hence seems to be associated with the upwelling water of the EUC. In the surface water,
13 *chlorophytes* and *Prochlorococcus* HL correlated positively with SST ($r_s = 0.13$, not
14 significant, and $r_s = 0.44$, significant) and negatively with SSS ($r_s = -0.15$, not significant, and
15 $r_s = -0.39$, significant). They were associated with warmer and less salty water masses than
16 *chrysophytes*, *dinoflagellates* and *haptophytes*. Thus, they were found predominantly north of
17 the equator. *Prochlorococcus* HL dominate among the species occurring from the surface
18 down to 50 m. *Prochlorococcus* LL, only observed in deeper layers (not shown here), were
19 the most abundant group from about 75 m downwards in the water column. These results are
20 in agreement with Johnson et al. (2006), where it was shown that *Prochlorococcus* dominate
21 in oligotrophic tropical waters, especially where nutrient concentrations are low at high
22 temperatures (between 15° S and 15° N of the Atlantic Ocean).

23

24 **4 Results**

25 **4.1 Surface water**

26 **4.1.1 CHBr₃ and CH₂Br₂**

27 Large regional variations were observed for the bromocarbons, especially for CHBr₃ in
28 surface water of the tropical Atlantic with a mean of $12.9 (1.8 - 44.7) \text{ pmol L}^{-1}$, and of 3.7
29 $(0.9 - 9.2) \text{ pmol L}^{-1}$ for CH₂Br₂ (Figure 2, Table 1). Concentrations from the underway
30 measurements and from the shallowest profile depths (<10m) were included in the evaluation
31 of the surface water concentrations. The observed values are in agreement with data from the
32 tropical oligotrophic Atlantic north of 16° N and the Mauritanian upwelling ranging between
33 1.0 and 43.6 for CHBr₃ and $0.6 - 9.4 \text{ pmol L}^{-1}$ for CH₂Br₂ with the largest values close to the
34 coast and the upwelling (Quack et al., 2007a; Carpenter et al., 2009; Hepach et al., 2014).

1 Quack et al. (2004) observed lower CHBr_3 of 2.3 pmol L^{-1} and CH_2Br_2 of 0.2 pmol L^{-1} at
2 10° N through the tropical Atlantic in boreal fall and values of 12.8 and 5.3 pmol L^{-1} for
3 CHBr_3 and CH_2Br_2 at the equator in agreement with our study. Values of up to 10 pmol L^{-1}
4 (CHBr_3) and 3 pmol L^{-1} (CH_2Br_2) near the equator were reported by Liu et al. (2013b). The
5 latter study covers the region during October and November, indicating that the equatorial
6 Atlantic seems to be a larger source for bromocarbons during the intense cooling in the
7 summer months. Both compounds show the same pattern in surface water throughout the
8 MSM18/3 cruise with hot spots slightly south of the equator.

9 The very good correlation between CHBr_3 and CH_2Br_2 is in agreement with studies from
10 several regions, mostly attributed to related sources for both compounds from macro- and
11 microalgae (Nightingale et al., 1995; Moore et al., 1996; Schall et al., 1997; Laturnus, 2001;
12 Quack et al., 2007b; Karlsson et al., 2008). Significant correlations to SST, SSS and TChl *a*
13 were found for CHBr_3 and CH_2Br_2 , while very low insignificant correlations were observed
14 with the 10 min averaged global radiation values (Table 2). The strongest correlations were
15 found to *Prochlorococcus* HL with $r_s = -0.70$ for CHBr_3 and -0.57 for CH_2Br_2 , and to
16 *chrysophytes* with $r_s = 0.43$, and $r_s = 0.41$, respectively.

17 **4.1.2 CH_3I and CH_2I_2**

18 The second highest mean sea surface water concentration was observed for CH_3I of 5.5 ($1.5 -$
19 12.8) pmol L^{-1} (Figure 2, Table 1), which is in the range of earlier studies. These studies were
20 widely spread in the region from 20° S to 25° N between the coasts of South America and
21 Africa with values between 0 and 36.5 pmol L^{-1} (Happell and Wallace, 1996; Schall et al.,
22 1997; Richter and Wallace, 2004; Jones et al., 2010; Hepach et al., 2014). 7.1 to 16.4 pmol L^{-1}
23 were detected in the vicinity of our investigated region (Richter and Wallace, 2004). CH_2I_2
24 was characterized by the lowest sea surface water concentrations of 1.1 ($0.3 - 3.7$) pmol L^{-1}
25 during MSM18/3. Literature reports of CH_2I_2 in the tropical Atlantic are very sparse: Schall
26 et al. (1997) report on average three times higher values of 3.4 ($2.1 - 6.8$) pmol L^{-1} in the
27 tropical Atlantic, while Jones et al. (2010) measured a five times higher mean of 5.8 (0.9 and
28 17.1) pmol L^{-1} (reported in Ziska et al. (2013)) in the northern tropical Atlantic.

29 Similar to CHBr_3 and CH_2Br_2 , sea surface CH_3I was significantly anticorrelated with SST
30 ($r_s = -0.42$) and not correlated with global radiation (Table 2). In contrast to the
31 bromocarbons, correlations were neither found to SSS, nor to latitude. Additionally, sea
32 surface CH_3I correlated to biomass indicators (TChl *a*: $r_s = 0.36$). The regional distribution of
33 CH_3I often followed qualitatively that of *haptophytes* ($r_s = 0.39$) with the most elevated
34 concentrations south of the equator. Positive correlations were also found to *dinoflagellates*

1 ($r_s = 0.29$) and *chrysophytes* ($r_s = 0.26$). A weak, but significant anticorrelation was observed
2 to wind speed ($r_s = -0.22$). In contrast to the other three halocarbons, CH_2I_2 was positively
3 correlated with SST ($r_s = 0.33$), and elevated concentrations were observed mostly north of
4 the equator. A weak negative correlation of CH_2I_2 was found with global radiation
5 ($r_s = -0.25$), indicating higher sea surface CH_2I_2 during the night time and lower
6 concentrations during the day. CH_2I_2 correlated both with *chlorophytes* ($r_s = 0.32$) and
7 *Prochlorococcus* HL ($r_s = 0.27$).

8 **4.2 Water column**

9 **4.2.1 CHBr_3 and CH_2Br_2**

10 CHBr_3 and CH_2Br_2 showed maxima at the surface, in the of the mixed layer and below it
11 (Figure 3, Table 3). The highest deep maximum concentrations of both CHBr_3 (up to 19.2
12 pmol L^{-1}) and CH_2Br_2 (up to 10.6 pmol L^{-1}) were observed in profile 4. At stations where
13 CHBr_3 was most elevated at the surface (profiles 2, 7, 12, 13), much higher overall CHBr_3
14 concentrations of up to 35.0 pmol L^{-1} were measured. CH_2Br_2 only reached maximum values
15 of up to 6.6 pmol L^{-1} in the surface (profiles 2, 7).

16 In contrast to surface water, CHBr_3 and CH_2Br_2 were distributed differently in the water
17 column with CH_2Br_2 being elevated 10 m below CHBr_3 in several profiles (Figure 3e). This
18 can also be seen in the T-S diagrams of these compounds (Figure 4a, b): while the most
19 elevated CHBr_3 was observed in the density layers between 1024 and 1025 kg m^{-3} (shallower
20 central water of the EUC), CH_2Br_2 was often also elevated in the denser, deeper layers below
21 30 m (Table 3). The maxima of both compounds were mostly in the vicinity of the TChl *a*
22 maximum. Results of the PCA (Figure 5) also show the dissimilarity of CHBr_3 and CH_2Br_2 at
23 depth: while the variance of CHBr_3 seems comparable to salinity and several phytoplankton
24 groups such as *chrysophytes*, CH_2Br_2 shows many similarities with the distribution of CH_2I_2
25 in the water column.

26 **4.2.2 CH_3I and CH_2I_2**

27 In agreement with CHBr_3 and CH_2Br_2 , CH_3I was elevated in the surface (three profiles 4, 6, 7)
28 (Table 4, Figure 3b) with values of up to 12.8 pmol L^{-1} , and also elevated in the deeper layers
29 in and below the mixed layer (Figure 3f), reaching up to 8.5 pmol L^{-1} . Most maxima of CH_3I
30 were observed closer to the surface within the mixed layer (Figure 4d). The PCA of CH_3I
31 revealed that its variance was similar to the variance of *dinoflagellates* and temperature
32 (Figure 5).

33 CH_2I_2 was always depleted in the surface. Maxima of CH_2I_2 were found in different depths,
34 sometimes associated with the TChl *a* maximum (Figure 3f), and mostly below the mixed

1 layer (Figure 3j). The maxima in deeper depths appeared concurrently with the deeper CH₂Br₂
2 maxima (Figure 4), which is also expressed in the PCA (Figure 5). Values were generally
3 much higher in deeper depths with e.g. 13.8 pmol L⁻¹ between 60 and 100 m at profile 5. The
4 highest concentrations of the whole cruise of 16.0 pmol L⁻¹ (profile 1) were found between 30
5 and 60 m. Concentrations of only up to 12.0 pmol L⁻¹ were found between 0 and 30 m (profile
6 6) (Table 4).

7 **4.3 Fluxes**

8 **4.3.1 CHBr₃ and CH₂Br₂**

9 Sea-to-air fluxes of CHBr₃ and CH₂Br₂ of 644 (-146 – 4285) and 187 (-3 – 762) pmol m⁻² h⁻¹
10 during MSM18/3 were larger during the first two western NS-transects of the cruise which
11 were characterized by higher seawater concentrations, as well as higher wind speeds (Table 1,
12 Figure 6). Carpenter et al. (2009) and Hepach et al. (2014) reported -150 and 3504
13 pmol m⁻² h⁻¹ CHBr₃ fluxes as well as of 5 – 917 for CH₂Br₂ from the Cape Verde and
14 Mauritanian upwelling region. The lower fluxes in the equatorial region are a result of the
15 lower wind speeds measured during MSM18/3, ranging from 0.3 – 11.1 with a mean of 6.1
16 m s⁻¹, and the lower concentration gradients in comparison to Carpenter et al. (2009). Quack
17 et al. (2004) reported CHBr₃ fluxes from the equatorial Atlantic of 2700 (± 800) pmol m⁻² h⁻¹,
18 which compare well to this study.

19 Diapycnal fluxes are the fluxes of halocarbons that diffuse out or into the mixed layer from
20 below the thermocline. Maxima within the mixed layer will lead to fluxes towards the
21 thermocline, while maxima below the mixed layer will result in a flux of halocarbon-
22 molecules into the mixed layer. Diapycnal fluxes of halocarbons were generally low although
23 the EUC can lead to enhanced mixing. This is due to the comparably small concentration
24 gradients of the halocarbons. Diapycnal fluxes were 80 (CHBr₃) to 200 times (CH₂Br₂) lower
25 than sea-to-air fluxes (Table 5). They acted both as a source and a sink for halocarbons in the
26 mixed layer. At eight stations, CHBr₃ was diffusing into the mixed layer, providing on
27 average 5 (0 – 14) pmol m⁻² h⁻¹ from below to the mixed layer budget of CHBr₃. On the other
28 hand, on average 30 (2 – 125) pmol m⁻² h⁻¹ were diffusing out of the mixed layer, which is the
29 highest flux to the thermocline of all four halocarbons, as a result of its large concentration
30 gradients across the bottom of the mixed layer. Diapycnal fluxes of CH₂Br₂ were generally
31 lower than for CHBr₃ due to its lower concentration gradients. Its fluxes into the mixed layer
32 from eight profiles were on average 3 (0 – 8) pmol m⁻² h⁻¹, while the diapycnal flux reduced
33 the mixed layer budget of CH₂Br₂ by 2 (0 – 8) pmol m⁻² h⁻¹ at the remaining five stations.

1 **4.3.2 CH₃I and CH₂I₂**

2 CH₃I sea-to-air fluxes were on average 425 (34 – 1300) pmol m⁻² h⁻¹ during the cruise. During
3 the eastern NS-transects, fluxes were elevated at several locations mostly during daytime in
4 contrast to the bromocarbons, in accordance to a larger concentration gradient of CH₃I in that
5 region (Table 1, Figure 6). The fluxes are only half of the sea-to-air fluxes from the equatorial
6 Atlantic region reported by Richter and Wallace (2004) of 958 ± 750 pmol m⁻² h⁻¹ and a fifth
7 of the fluxes reported from Jones et al. (2010) of on average 2154 pmol m⁻² h⁻¹ from the Cape
8 Verde and Mauritanian upwelling region. But, they were two times larger than the fluxes of
9 Hepach et al. (2014) of on average 246 pmol m⁻² h⁻¹. CH₂I₂ fluxes were generally larger in the
10 beginning of the cruise where higher wind speeds and higher surface water concentrations
11 existed. Only few studies have published sea-to-air fluxes of CH₂I₂ from the tropical ocean.
12 CH₂I₂ emissions calculated for MSM18/3 are with only 82 (3 – 382) pmol m⁻² h⁻¹ very low in
13 comparison to mean fluxes reported by Jones et al. (2010) of on average 541 –
14 688 pmol m⁻² h⁻¹, which are the result of higher oceanic CH₂I₂ (Jones et al., 2010).
15 Similar to the bromocarbons, diapycnal fluxes of CH₃I and CH₂I₂ were generally lower (117
16 and 7 times, respectively) than sea-to-air fluxes (Table 5). Due to the larger CH₃I
17 concentrations in the mixed layer compared to the upper thermocline, diapycnal fluxes of 5 (1
18 – 13) pmol m⁻² h⁻¹ were mostly acting as a sink for the mixed layer budget. Only at three
19 stations, 2 (1 – 5) pmol m⁻² h⁻¹ were transported into the mixed layer. Diapycnal fluxes of
20 CH₂I₂ acted mostly as source for the mixed layer, providing on average 12 (0 –
21 39) pmol m⁻² h⁻¹ due to its much higher concentrations in the water below. This represents the
22 highest halocarbon flux of the four compounds into the mixed layer. The diapycnal flux of
23 CH₂I₂ of 2 (0 – 4) pmol m⁻² h⁻¹ out of the mixed layer was only observed at three stations.

24

25 **5 Discussion**

26 **5.1 Surface water distribution**

27 **5.1.1 CHBr₃ and CH₂Br₂**

28 The equatorial Atlantic is a source of CHBr₃ and CH₂Br₂ to the atmosphere during the ACT
29 season, and the correlations of their water concentrations to biogenic parameters indicate
30 biological formation. CHBr₃ and CH₂Br₂ correlated significantly, but weakly with TChl *a*,
31 which is not an unusual feature (Abrahamsson et al., 2004a; Carpenter et al., 2009; Liu et al.,
32 2011; Hepach et al., 2014). It has been suggested that CHBr₃ is not produced directly from
33 phytoplankton, but rather from dissolved organic matter (DOM) present in sea water (Lin and
34 Manley, 2012). This was more closely investigated in laboratory experiments by Liu et al.

1 (2015), who suggested that the weak in-situ correlations of bromocarbons with Chl *a* are a
2 result of this indirect production pathway. The correlation with certain phytoplankton groups
3 may then be caused by the production of phytoplankton-specific DOM. The very negative
4 correlations of bromocarbons with SST and positive correlations with SSS indicate a
5 relationship of bromocarbon abundance with processes within the cold and nutrient-rich
6 upwelled water of the EUC (section 3.2), supported by the T-S diagrams (Figure 4). Weak,
7 but significant negative correlations with latitude ($r_s = -0.38$ for CHBr_3 and $r_s = -0.18$ for
8 CH_2Br_2) and maximum values of the bromocarbons between 2 and 3° S, where EUC water
9 reaches the surface, underline this hypothesis. Although the correlation analysis of
10 halocarbons with phytoplankton groups cannot directly resolve production and loss processes
11 by algal activity, it is still an indicator for possible involvement of these species in halocarbon
12 production. Bromocarbon production might exceed loss processes, which leads to the
13 observed statistical link of CHBr_3 and CH_2Br_2 to *chrysophytes*. *Chrysophytes* are to our
14 knowledge not yet among observed halocarbon producers in incubation and field studies. The
15 strong negative correlations of *Prochlorococcus* HL with CHBr_3 and CH_2Br_2 have been
16 observed previously (Hepach et al., 2014). These significant negative correlations can be
17 explained by the large abundance of *Prochlorococcus* in warm water while bromocarbons on
18 the other hand are more correlated with the cooler water of the EUC, which is richer in
19 nutrients and *chrysophytes*, *haptophytes* and *dinoflagellates*.

20 **5.1.2 CH_3I and CH_2I_2**

21 CH_3I concentrations and wind speed were weakly anticorrelated during MSM18/3. Richter
22 (2004) interprets this as depletion of the surface concentrations, when air-sea fluxes exceed
23 the production rate during high wind speed. There are two production mechanisms suggested
24 for CH_3I . Previous studies (Richter and Wallace, 2004; Jones et al., 2010) have attributed
25 CH_3I in the tropical ocean mainly to photochemical formation based on the observations of
26 Moore and Zafiriou (1994). In contrast to these studies, indications for biological formation of
27 CH_3I were found in the ACT region during our study. CH_3I showed a weak negative
28 correlation with SST, significant correlations with the biologically produced CHBr_3 and
29 CH_2Br_2 (Table 2) and with TChl *a* as biomass indicator, and no correlation to global radiation.
30 These imply a relationship with the biologically active upwelled water. Elevated
31 concentrations of CH_3I were found between 10° and 5° W during midday (see CH_3I in
32 comparison to global radiation in Figure 2), which could be a result of photochemical
33 formation. Thus we suggest that photochemistry and biological production likely both played
34 a role during MSM18/3. *Haptophytes* correlated most significantly of the phytoplankton

1 groups with CH₃I and have already been shown to produce CH₃I both in the laboratory (Itoh
2 et al., 1997; Manley and de la Cuesta, 1997; Scarratt and Moore, 1998; Smythe-Wright et al.,
3 2010) and in the field (Abrahamsson et al., 2004b). Correlations during MSM18/3
4 additionally indicate a possible involvement of *dinoflagellates* and *chrysophytes* in the
5 production of methyl iodide (Table 2). The importance of oceanic CH₃I production by
6 *Prochlorococcus* is a matter of dispute. Brownell et al. (2010) report it to be a minor
7 source, in contrast to both Smythe-Wright et al. (2006) and Hughes et al. (2010, 2011). No
8 evidence of involvement of *Prochlorococcus* HL was found during MSM18/3.

9 The very low sea surface concentrations of CH₂I₂ with lowest concentrations during the day
10 can be explained by its fast photolysis (few minutes lifetime in surface sea water) (Jones and
11 Carpenter, 2005; Martino et al., 2005). Although CH₂I₂ is generally assumed to be of biogenic
12 origin in the open ocean (Moore and Tokarczyk, 1993; Yamamoto et al., 2001; Orlikowska
13 and Schulz-Bull, 2009; Hopkins et al., 2013), great uncertainties remain as to which species
14 are involved in its production. During MSM18/3, indications were found for different source
15 species than of the other three compounds (*chlorophytes* and *Prochlorococcus* HL).

16 **5.2 Water column distribution**

17 Halocarbon maxima in the TChl *a* maximum, attributed to their biological production, are
18 often observed from polar to tropical regions (Moore and Tokarczyk, 1993; Moore and
19 Groszko, 1999; Yamamoto et al., 2001; Quack et al., 2004; Carpenter et al., 2007; Hughes et
20 al., 2009). In contrast, photochemical formation of CH₃I can lead to surface maxima (Happell
21 and Wallace, 1996). During MSM18/3, maxima of halocarbons were not always found in the
22 TChl *a* maximum. This does not contradict their biological production, as the location of the
23 TChl *a* maximum is not necessarily the location of highest biomass or primary production, but
24 rather reflects the photoadaptation capability of the predominant phytoplankton groups
25 (Claustre and Marty, 1995). Unfortunately, neither biomass nor primary production was
26 measured during the cruise. Additionally, halocarbons could be produced by phytoplankton
27 groups that are not in the maximum of the biomass distribution in the water column, and the
28 location of the halocarbon maximum might be more determined from their sink processes
29 than from their production. Surprisingly, the time of day, influencing sink and production
30 processes, seemed to play a minor role for the shape of the profiles for all four compounds
31 (see the location of the CTD stations in Fig. 2).

32 **5.2.1 CHBr₃ and CH₂Br₂**

33 In contrast to their similar occurrence in the surface, CHBr₃ and CH₂Br₂ showed different
34 distributions in the water column (Figure 5). Strong indications for biological sources of

1 CHBr₃ exist in the PCA, and *chrysophytes* as potential source group are in agreement to the
2 surface water observations (Table 2, Figure 5). Maximum CH₂Br₂ concentrations were
3 occasionally found below the CHBr₃ maxima, which have already been observed in the
4 Mauritanian upwelling (Quack et al., 2007b). The deeper maxima may be either due to an
5 additional source of CH₂Br₂ such as the biologically mediated conversion of CHBr₃ (Hughes
6 et al., 2013) or to a faster degradation of CHBr₃ than of CH₂Br₂ at depth. Sinks for CHBr₃ and
7 CH₂Br₂ in tropical surface waters include very slow hydrolysis (hundreds to thousands of
8 years) (Mabey and Mill, 1978) and slow halogen substitution (5 years) (Geen, 1992).
9 Photolysis, which has been suggested to be faster for CHBr₃ (9 years with a mixed layer of
10 100 m for CHBr₃) than for CH₂Br₂ (Carpenter et al., 2009) would be of more significance in
11 the surface layer. A faster degradation of CHBr₃ in greater depths is also somewhat contrary
12 to the observed very fast bacterial degradation of CH₂Br₂ with a half-life of 2 days (Goodwin
13 et al., 1998). An additional source for CH₂Br₂ that involves CHBr₃ therefore seems more
14 plausible. At four of the 13 stations, indications for the additional source were found. There,
15 maximum CH₂Br₂ concentrations were found below CHBr₃, which could be the result of its
16 faster conversion to CH₂Br₂ than its production. CH₂Br₂ in denser water is also co-located
17 with *Prochlorococcus* LL, which might be involved in the CHBr₃-conversion.

18 **5.2.2 CH₃I and CH₂I₂**

19 CH₃I was usually elevated in the top 30 m of the water column apart from three profiles,
20 where maximum concentrations were found between 30 and 60 m. The surface maxima, as
21 seen in the T-S diagram (Figure 4), support the photochemical formation of CH₃I (Happell
22 and Wallace, 1996). Deeper maxima could also arise if the sea-to-air flux exceeds the
23 photochemical production. However, the low wind speed during the cruise (section 3), the
24 relationship with biological parameters, and the partly co-located maxima with the other three
25 biogenic halocarbons (Figure 3, Figure 5) also point to a direct production of CH₃I from
26 phytoplankton. These include *dinoflagellates* as indicated by the correlations and the PCA
27 (Figure 5).

28 CH₂I₂ was always depleted in the surface with respect to the underlying water column as a
29 result of its strong photolysis (Jones and Carpenter, 2005; Martino et al., 2006). It was
30 frequently elevated below the TChl *a* maximum and below the base of the mixed layer
31 (Figure 3) in contrast to previous studies (Moore and Tokarczyk, 1993; Yamamoto et al.,
32 2001). The similarity in its distribution to CH₂Br₂ (Figure 4, Figure 5) could indicate similar
33 production and sink processes at depth. Bacterial formation of CH₂I₂ (Fuse et al., 2003;
34 Amachi et al., 2005) in the upper thermocline could also be an additional source for this

1 compound. Alternatively, CH_2I_2 may not degrade as quickly as CHBr_3 and CH_3I in greater
2 depths, which would lead to its accumulation below the mixed layer.

3 **5.3 Factors contributing to halocarbon emissions from the mixed layer**

4 Halocarbon emissions into the atmosphere depend strongly on the mixed layer budget of these
5 compounds, which is determined by their sources and sinks. It is unclear, where the main
6 halocarbon production occurs. It has been suggested that it takes mainly place in the
7 subsurface TChl *a* maximum (Quack et al., 2004; Martino et al., 2006), whereas other model
8 studies assume production of e.g. CHBr_3 to be coupled to primary production in the whole
9 water column (Hense and Quack, 2009). Assuming production of halocarbons takes place
10 mainly in the TChl *a* maximum, which is often located below the mixed layer, diapycnal
11 fluxes from below the thermocline will be the most important source for mixed layer
12 halocarbons.

13 **5.3.1 Transport and loss processes in the mixed layer**

14 To evaluate the significance of halocarbon production below the mixed layer for emissions
15 into the atmosphere, production, loss and transport processes have to be considered. The
16 diapycnal fluxes of the four halocarbons were calculated from 13 halocarbon profiles and
17 parallel measurements of eddy diffusivity (section 4.3). The data are characterized by a low
18 depth resolution of the halocarbons within the water column and a short validity of the
19 diffusion coefficients, which make the diapycnal fluxes subject to some uncertainties. Given
20 that the depth profiles measured during MSM18/3 agree well to previous studies from the
21 tropical ocean (Yamamoto et al., 2001; Quack et al., 2004), a general idea of the significance
22 of diapycnal fluxes for the mixed layer budget of halocarbons can be obtained. The chemical
23 loss rates are estimated from published data which include hydrolysis, halogen substitution
24 and photolysis. The half-lives of CHBr_3 and CH_2Br_2 due to hydrolysis are hundreds to
25 thousands of years (Mabey and Mill, 1978), while for CH_3I , the half-life due to hydrolysis
26 ranges from 1600 days at 25 °C to 4000 days at 5 °C (Elliott and Rowland, 1995). The half-
27 life of CHBr_3 with respect to photolysis is 9 years assuming a mixed layer depth of 100 m and
28 is potentially slower for CH_2Br_2 (Carpenter and Liss, 2000), halogen-substitution is 5 years in
29 warm waters (Geen, 1992). Liu et al. (2011) calculated the half-life of CHBr_3 due to
30 photolysis in a coastal mixed layer of 5 m to be only 82 days. Mixed layers during MSM18/3
31 were from down to 49 m, photolysis of bromocarbons in the mixed layer will lead to half-
32 lives of several months. Sea-to-air flux is the most significant sink for CHBr_3 and CH_2Br_2
33 from the mixed layer. Mean half-lives of 8 days were calculated for both compounds during
34 MSM18/3, based on the fluxes (section 4.3.1) and the mixed layer depths during the cruise

1 (Table 3). We consider a very short time scale of 1 h for our budget calculations due to the
 2 validity of the diapycnal flux coefficients, while the general findings of our calculations are
 3 also valid for a longer time scale. As the sink from the mixed layer due to sea-to-air fluxes is a
 4 magnitude larger than the other mentioned sinks, we will neglect them in our estimates for
 5 CHBr_3 and CH_2Br_2 as they do not play a large role. Photolysis of CH_3I is very slow in
 6 comparison to halide substitution (Zika et al., 1984). The latter is suggested to be an important
 7 sink in the tropical ocean during low wind speeds (Jones and Carpenter, 2007), while large
 8 wind speeds favor sea-to-air fluxes as main sink (mean half-life of 8 days during MSM18/3).
 9 All three sink processes are included in our budget estimates using the rates published by
 10 Elliott and Rowland (1993). For CH_2I_2 , photolysis is the most significant sink in surface water
 11 (Jones and Carpenter, 2005). In our calculations, losses of CH_2I_2 due to photolysis were
 12 calculated according to Martino et al. (2006) with a photon flux calculated from the NASA
 13 COART model (Jin et al., 2006), a TChl *a* concentration of $0.4 \mu\text{g L}^{-1}$, absolute quantum
 14 yields from Martino et al. (2006), and absorption cross sections determined by Jones and
 15 Carpenter (2005).

16 **5.3.2 Mixed layer budget of halocarbons during MSM18/3**

17 In the following section, the results of the halocarbon budget calculations are presented. The
 18 total mixed layer concentrations were calculated at every station considering a water column
 19 with a volume of $1 \times 1 \times z_{ML} \text{ m}^3$. Assuming that halocarbons are only produced below the
 20 mixed layer, the following relationship (equation 4) is valid for the steady state concentration
 21 C_{hal} , with F_{dia} and F_{adv} as the source terms from diapycnal fluxes and advection, while S_{as}
 22 (Figure 6) and S_{ch} represent the loss terms sea-to-air flux and chemical sinks as described in
 23 the previous section:

$$24 \quad C_{hal} = F_{dia} + F_{adv} - S_{as} - S_{ch} \quad (4)$$

25 S_{as} is the main sink term for CHBr_3 , CH_2Br_2 and CH_3I during MSM18/3 (Table 6). On the
 26 short time scales considered here, diapycnal fluxes of CH_3I , which can reduce the mixed layer
 27 by around 5 pmol per hour (Table 5), compete with the loss due to chloride substitution (S_{ch}).
 28 For CH_2I_2 , S_{ch} (photolysis) is about 10 times higher than S_{as} , and reduces the mixed layer
 29 budget by 24 % after 1 h. In total, diapycnal fluxes (F_{dia}) into the mixed layer were not
 30 sufficient to account for the losses of all four compounds from the mixed layer (Table 6). The
 31 discrepancies with respect to the total mixed layer are 169 (CH_2Br_2), 255 (CH_3I), 269
 32 (CHBr_3) to 8382 (CH_2I_2) pmol h^{-1} , which are small compared to the total amount of
 33 halocarbons in the mixed layer (CHBr_3 – 0.17 %, CH_2Br_2 – 0.19 %, CH_3I – 0.34 %, CH_2I_2 –
 34 13.11 %). Possible reasons for the observed discrepancies are evaluated in the following.

1 Advection of the missing halocarbons, F_{adv} , likely does not play a large role for CH_2Br_2 , CH_3I
 2 and CH_2I_2 , since mean mixed layer concentrations of these compounds were rather
 3 homogeneous in the whole region. Thus, only for CHBr_3 , with more variable concentrations,
 4 advection may transport significant amounts from one location to another. In addition,
 5 halocarbon maxima were found within the mixed layer, which may either result from a mixed
 6 layer that is not well mixed or halocarbon production is faster than mixing in the mixed layer.
 7 According to the temperature and salinity profiles during the whole cruise (Figure 3), the
 8 mixed layer was very well mixed. Consequently, production in the mixed layer is the most
 9 likely process balancing the missing halocarbons (Table 6) as diapycnal fluxes and advection
 10 play minor roles. The maxima that occasionally evolve in the mixed layer suggest that
 11 production of halocarbons is rapid, but may vary with depth. The mixed layer production
 12 term, here called P_{ML} , has to be included in the budget calculation of equation 4:

$$13 \quad C_{hal} = F_{dia} + F_{adv} - S_{as} - S_{ch} + P_{ML} \quad (5)$$

14 The relative production of halocarbons in the mixed layer is likely largest for CH_2I_2 , because
 15 its largest discrepancy arises from its rapid photolysis (up to 24 % loss in 1 h) (Table 6). This
 16 is in agreement to earlier studies investigating macroalgal production, proposing larger release
 17 rates of CH_2I_2 than of CHBr_3 , CH_2Br_2 and CH_3I (Klick and Abrahamsson, 1992; Carpenter et
 18 al., 2000).

19 **5.3.3 Production rates of halocarbons**

20 From the budget calculations, described in the previous section, potential production rates P_{ML}
 21 for the mixed layer are determined for each station. The mean production rates show large
 22 standard deviations (Table 7), including the variability and uncertainties in the estimated
 23 production rates. Production rates are 34 ± 65 (CHBr_3), 10 ± 12 (CH_2Br_2), 21 ± 24 (CH_3I),
 24 and 384 ± 318 $\text{pmol m}^{-3} \text{ h}^{-1}$ (CH_2I_2). These are the first estimated production rates of CHBr_3
 25 and CH_2Br_2 for tropical phytoplankton species. For comparison to other studies, the
 26 production rates from this study are converted to rates per $\mu\text{g TChl } a$ (reported in Tables 3
 27 and 4), which results in mean (\pm standard deviation) production rates of $2.5 \times 10^{-3} \pm 4.5 \times 10^{-3}$
 28 (CHBr_3), $8.4 \times 10^{-4} \pm 1.0 \times 10^{-3}$ (CH_2Br_2), $2.2 \times 10^{-3} \pm 3.0 \times 10^{-3}$ (CH_3I) and $3.3 \times 10^{-2} \pm 3.3 \times$
 29 10^{-2} $\text{pmol} [\mu\text{g TChl } a]^{-1} \text{ h}^{-1}$ (CH_2I_2).

30 **5.3.4 Comparison to previously reported rates – CHBr_3 and CH_2Br_2**

31 Tokarczyk and Moore (1994) and Hughes et al. (2013) determined production rates from
 32 polar algae in laboratory studies ranging between 2×10^{-3} and 2.1×10^{-2} $\text{pmol} [\mu\text{g Chl } a]^{-1} \text{ h}^{-1}$
 33 on average for CHBr_3 , depending on the growth phase, which is in the range of our calculated
 34 rates. Production rates for CH_2Br_2 of on average $2.1 - 4.2 \times 10^{-3}$ $\text{pmol} [\mu\text{g Chl } a]^{-1} \text{ h}^{-1}$ were

1 much higher than the ones calculated in our study (Tokarczyk and Moore, 1994). Karlsson et
2 al. (2008) published production rates of $2.6 - 9.3 \times 10^{-2}$ pmol [$\mu\text{g Chl a}$] $^{-1}$ h $^{-1}$ for CHBr₃
3 (depending on the time of day) and $5 \times 10^{-4} - 3.6 \times 10^{-3}$ pmol [$\mu\text{g Chl a}$] $^{-1}$ h $^{-1}$ for CH₂Br₂ from
4 an in situ study in the Baltic Sea during a cyanobacterial bloom. Liu et al. (2011) calculated
5 417 (CHBr₃) and 258 pmol m $^{-3}$ h $^{-1}$ (CH₂Br₂) for the subtropical and temperate eastern US
6 coast, which are tenfold higher than the production rates determined from our study (Table 7).
7 The differences between these studies and ours may have several origins. Taking an average
8 production rate for the total mixed layer during MSM18/3 does not take a potential variable
9 production with depth into account. Second, the different production rates determined in the
10 monocultural studies (Tokarczyk and Moore, 1994; Hughes et al., 2013) show large variations
11 between different types of microalgae. Third, the indirect estimates during MSM18/3 are
12 afflicted by the uncertainties in the individual budget terms, which are also expressed in the
13 large standard deviations.

14 **5.3.5 Comparison to previously reported rates – CH₃I and CH₂I₂**

15 Production rates of CH₃I determined from *Prochlorococcus* vary significantly from 5.8×10^{-4}
16 to 9.4×10^{-2} pmol [$\mu\text{g Chl a}$] $^{-1}$ h $^{-1}$ (Smythe-Wright et al., 2006; Brownell et al., 2010). Hughes
17 et al. (2011) suggested this variability to be caused by different cell states, e.g. healthier cells
18 producing less CH₃I. While Scarratt and Moore (1999) determined rates from $8.3 \times 10^{-3} - 5.0$
19 $\times 10^{-2}$ pmol [$\mu\text{g Chl a}$] $^{-1}$ h $^{-1}$ from a red microalgal species, Karlsson et al. (2008) reported a
20 rate of 1.0×10^{-2} pmol CH₃I [$\mu\text{g Chl a}$] $^{-1}$ h $^{-1}$ from a cyanobacterial bloom in the Baltic Sea,
21 which is at the higher end of the range mentioned here. Our estimates lie well within these
22 cited ranges of phytoplankton production rates and are thus a reasonable assumption for the
23 CH₃I production strength of tropical algae (see section 5.1.2).

24 In contrast to the other three halocarbons, very few studies have actually determined
25 production rates of CH₂I₂ from phytoplankton. CH₂I₂ was shown to be produced in
26 comparatively larger concentrations than other halocarbons, but generally from fewer species
27 (six polar and temperate *diatom* species were tested, of which only two produced CH₂I₂)
28 (Moore et al., 1996). Martino et al. (2006) assumed a theoretical production rate of 17,000
29 pmol m $^{-3}$ h $^{-1}$ in the tropical equatorial Atlantic. These were calculated from previously
30 reported CH₂ClI fluxes based on the assumption that CH₂ClI is mainly formed during the
31 photolysis of CH₂I₂ and that CH₂I₂ is only produced in the TChl *a* maximum. This rate
32 appears very large in comparison to our estimate and in comparison to the production rates of
33 the other halocarbons. We showed evidence that CH₂I₂ is not only produced within the TChl *a*
34 maximum but in the whole mixed layer, thus, lower average production rates seem more

1 plausible. CH₂I₂ together with CH₂ClI have been suggested to be equally important carriers of
2 organoiodine into the troposphere (Saiz-Lopez et al., 2012), hence it is important to determine
3 specific phytoplankton production rates of CH₂I₂ in future studies.

4 Our calculated production rates of CHBr₃, CH₂Br₂ and CH₃I lie well within the ranges of
5 several laboratory and field studies of mostly temperate and polar algae, suggesting
6 production from tropical algae to be similarly significant. CH₂I₂ was shown to be produced in
7 larger rates than the other three compounds, but very rapid photolysis leads to lower sea
8 surface concentrations of this compound. However, considering the large ranges in reported
9 production rates of CHBr₃, CH₂Br₂, CH₃I and the lack of studies concentrating on CH₂I₂,
10 more incubation experiments are severely needed to constrain in situ production rates of
11 tropical algae. This information is crucial to evaluate the significance and contribution of the
12 tropical ocean with respect to halogen transport into the troposphere, and finally into the
13 stratosphere. Understanding the fate of halocarbons within the water column is an important
14 task to estimate their distribution and emissions from the future ocean.

16 **6 Summary and conclusions**

17 Increased biological production during the Atlantic Cold Tongue (ACT) caused elevated
18 CHBr₃ and CH₂Br₂ concentrations of up to 44.7 pmol L⁻¹ and up to 9.2 pmol L⁻¹ within the
19 equatorial surface water with comparable concentrations to other tropical upwelling systems.
20 Both compounds showed similar distributions and maxima in the region where the Equatorial
21 Undercurrent (EUC) influences the surface water between 2° and 3° S with cooler water and
22 elevated nutrients. *Chrysophytes*, the dominating phytoplankton group in the equatorial
23 surface water, were likely involved in the bromocarbon production. In contrast to their similar
24 surface water occurrence, CHBr₃ and CH₂Br₂ showed different distributions in the water
25 column. While CHBr₃ was mostly elevated in shallower layers in close proximity to the TChl
26 *a* maximum, CH₂Br₂ frequently showed maxima in deeper water likely caused by an
27 additional source.

28 In contrast to other tropical Atlantic regions, correlations of CH₃I with CHBr₃ and with
29 biological parameters indicate biogenic formation of CH₃I during the ACT. Moderate CH₃I
30 concentrations of up to 12.8 pmol L⁻¹ were measured in the surface water. CH₂I₂ surface water
31 and mixed layer concentrations were lowest due to its strong photolysis with maximum values
32 of only 3.7 pmol L⁻¹. CH₂I₂ maxima below the mixed layer, suggest similar formation
33 pathways to CH₂Br₂ possibly tied to heterotrophic activities below the layers of maximum
34 production.

1 Sea-to-air fluxes were the most important sink from the mixed layer of CHBr_3 , CH_2Br_2 and
2 CH_3I , while photolysis was the main sink for CH_2I_2 . For the first time, halocarbon turbulent
3 fluxes from and into the mixed layer were calculated using microstructure measurements and
4 halocarbon concentration gradients in the water column. The significance of these diapycnal
5 fluxes as a source for mixed layer halocarbons, suggested by halocarbon maxima below the
6 mixed layer, was evaluated in comparison to sea-to-air fluxes and other sinks. All sinks of
7 halocarbons from the mixed layer were much larger than the diapycnal supply into the mixed
8 layer. Hence, halocarbon production in the entire mixed layer is the most important factor
9 contributing to marine emissions of these compounds.

10 Production rates of halocarbons were estimated from 13 profiles for the tropical mixed layer.
11 Calculated production rates varied between the stations and were: $34 \pm 65 \text{ pmol m}^{-3} \text{ h}^{-1}$ for
12 CHBr_3 , $10 \pm 12 \text{ pmol m}^{-3} \text{ h}^{-1}$ for CH_2Br_2 , $21 \pm 24 \text{ pmol m}^{-3} \text{ h}^{-1}$ for CH_3I and $384 \pm 318 \text{ pmol}$
13 $\text{m}^{-3} \text{ h}^{-1}$ for CH_2I_2 with large variability between the different stations. These are generally in
14 the range of rates reported from both monocultural and in situ incubation studies for CHBr_3 ,
15 CH_2Br_2 and CH_3I , while CH_2I_2 seems to be emitted in larger concentrations from
16 phytoplankton.

17 Our results show the need to conduct more process-related studies in the field. The first
18 consideration of diapycnal mixing revealed that maximum concentrations in the vicinity of
19 the TChl *a* maximum are insignificant for the mixed layer budget. Investigating the exact
20 mechanisms of formation, degradation and transport of halocarbons in the water column
21 remains an important task toward understanding current and future emissions of these
22 compounds. Understanding the actual processes that contribute to their concentrations and
23 distribution within the water column is crucial to predict their emissions. We therefore
24 suggest further mono-cultural incubation studies to determine species-dependent production
25 and consumption rates. Temporally resolved in situ incubations in different depths within the
26 water column in combination with diapycnal flux measurements will help to explain the
27 profile shapes. Further halocarbon emission studies in the tropical ocean in different seasons
28 are crucial to evaluate their importance for the stratospheric halogen loading in a global
29 perspective.

30

31 **Acknowledgements**

32 We thank the chief scientist of the cruise MSM18/3 Arne Körtzinger, as well as the captain,
33 the crew and the scientific crew of RV *Maria S. Merian* for all of their help. The authors
34 acknowledge Sonja Wiegmann for pigment analysis, Bettina Taylor for CHEMTAX

1 calculations, and Martina Lohmann for nutrient measurements. We thank Björn Fiedler for
2 providing the fluorescence sensor data. We also appreciate the helpful input of Christa
3 Marandino. Additionally, the authors acknowledge NASA for providing satellite MODIS-
4 Aqua data of June and July 2011. This work was part of the German research project
5 SOPRAN II and III (grant no. FKZ 03F0611A and 03F0662A) funded by the
6 Bundesministerium für Bildung und Forschung (BMBF), and was also supported by the EU
7 project SHIVA (grant no. FP7-ENV-2007-1-226224) and by the HGF Innovative Network
8 Fund (PHYTOOPTICS project).

1

2 **Tables**

3 Table 1. Mean (minimum – maximum) values of physical parameters (sea surface temperature (SST), sea surface salinity (SSS), and wind
 4 speed), surface biomass proxies (TChl *a*–H: TChl *a* from HPLC measurements, TChl *a*–F: TChl *a* determined from the continuously
 5 measuring fluorescence sensor), and sea surface concentrations, as well as sea-to-air fluxes of the four halocarbons CHBr₃, CH₂Br₂, CH₃I, and
 6 CH₂I₂ during the cruise MSM18/3.

Parameter	SST	SSS	Wind speed	Biomass proxies		Halocarbons							
						CHBr ₃		CH ₂ Br ₂		CH ₃ I		CH ₂ I ₂	
				TChl <i>a</i> -H	TChl <i>a</i> -F	Concentrations	Sea-to-air fluxes	Concentrations	Sea-to-air fluxes	Concentrations	Sea-to-air fluxes	Concentrations	Sea-to-air fluxes
Unit	[° C]		[m s ⁻¹]	[µg L ⁻¹]	[pmol L ⁻¹]	[pmol m ⁻² h ⁻¹]	[pmol L ⁻¹]	[pmol m ⁻² h ⁻¹]	[pmol L ⁻¹]	[pmol m ⁻² h ⁻¹]	[pmol L ⁻¹]	[pmol m ⁻² h ⁻¹]	
Mean	24.4	35.7	6.1	0.51	0.44	12.9	644	3.7	187	5.5	425	1.1	82
Min	22.1	34.5	0.3	0.10	0.06	1.8	-146	0.9	-3	1.5	34	0.3	3
Max	29.0	36.3	11.1	0.99	1.20	44.7	4285	9.2	762	12.8	1300	3.7	382

7

1 Table 2. Spearman's rank correlation coefficients r_s of halocarbons with different physical parameters and phytoplankton species measured in
 2 surface water. Numbers printed in bold are regarded as significant with $p < 0.05$.

	CHBr ₃	CH ₂ Br ₂	CH ₃ I	CH ₂ I ₂	SST	Salinity	Global radiation	Latitude	Wind speed	Chlorophyll a + Div a	Chlorophytes	Chrysophytes	Dinoflagellates	Haptophytes
Prochlorococcus (HL)	-0.70	-0.57	-0.21	0.27	0.44	-0.39	-0.20	0.49	0.26	-0.01	0.34	-0.28	-0.14	-0.33
Haptophytes	0.34	0.37	0.39	-0.25	-0.58	0.34	0.16	-0.21	-0.34	0.57	-0.18	0.37	0.53	
Dinoflagellates	0.22	0.22	0.29	-0.02	-0.50	0.10	-0.14	-0.33	-0.37	0.72	0.09	0.40		
Chrysophytes	0.43	0.41	0.26	0.13	-0.45	0.48	-0.28	-0.15	-0.15	0.71	0.22			
Chlorophytes	-0.29	-0.26	-0.15	0.32	0.13	-0.15	-0.26	0.25	-0.05	0.11				
TChl a	0.23	0.27	0.36	0.04	-0.58	0.35	-0.22	-0.13	-0.27					
Wind speed	-0.18	-0.16	-0.22	0.20	0.56	-0.06	0.12	0.04						
Latitude	-0.38	-0.18	0.03	0.12	0.10	-0.20	-0.08							
Global radiation	0.05	0.04	-0.09	-0.25	0.19	-0.09								

SSS	0.48	0.41	-0.09	-0.04	-0.42
SST	-0.46	-0.46	-0.42	0.33	
CH ₂ I ₂	0.07	0.09	-0.04		
CH ₃ I	0.50	0.62			
CH ₂ Br ₂	0.90				

1
2 Table 3. Concentrations of CHBr₃, CH₂Br₂ and TChl *a* (from HPLC measurements) averaged over different depths at every CTD station (1 –
3 13), as well as the mixed layer depth. If a range is not given, only one measurement point exists. Bold numbers indicate the depth of
4 maximum concentrations at this station.

	0 – 30 m		31 – 60 m		61 – 100 m	
<i>z_{ML}</i> [m]	Concentrations [pmol L ⁻¹]		Concentrations [pmol L ⁻¹]		Concentrations [pmol L ⁻¹]	
	CHBr ₃	CH ₂ Br ₂	CHBr ₃	CH ₂ Br ₂	CHBr ₃	CH ₂ Br ₂

1	34	5.4 (3.2 - 6.5)	1.7 (1.3 - 2.1)	0.60 (0.52 - 0.69)	5.8 (3.7 - 7.9)	3.0 (1.8 - 4.2)	0.59 (0.53 - 0.65)	2.1	1.1	---
2	16	30.2 (25.4 - 35.0)	6.5 (6.4 - 6.6)	0.92 (0.76 - 1.07)	9.0 (7.6 - 10.3)	5.2 (5.1 - 5.4)	0.86 (0.74 - 0.97)	2.4 (1.2 - 4.6)	1.8 (0.8 - 3.6)	0.20 (0.10 - 0.30)
3	37	6.8 (6.2 - 7.4)	3.9 (3.6 - 4.2)	0.80 (0.75 - 0.86)	3.0 (2.6 - 3.2)	2.4 (2.4 - 2.5)	0.65 (0.51 - 0.80)	2.3 (2.2 - 2.5)	2.3 (2.3 - 2.3)	0.18
4	14	12.5 (5.8 - 19.2)	7.2 (3.8 - 10.6)	0.56 (0.26 - 0.86)	5.9 (4.8 - 6.9)	3.1 (3.0 - 3.2)	0.80 (0.79 - 0.81)	2.6 (2.0 - 3.2)	2.5 (1.8 - 3.2)	0.19 (0.13 - 0.26)
5	49	14.0 (13.6 - 14.4)	4.2 (4.0 - 4.3)	0.34 (0.28 - 0.39)	11.7	4.8	0.58	7.6 (6.6 - 8.5)	7.4 (6.1 - 8.6)	0.39 (0.24 - 0.53)
6	12	13.4 (12.5 - 14.3)	5.0 (3.8 - 6.3)	0.99	5.4 (5.1 - 5.7)	4.8 (4.7 - 4.8)	0.30 (0.17 - 0.43)	4.9 (4.7 - 5.1)	4.6 (4.6 - 4.7)	0.10 (0.04 - 0.17)
7	---	11.2 (8.8 - 13.7)	4.6 (3.5 - 4.6)	0.71 (0.65 - 0.76)	3.7 (2.5 - 4.9)	3.4 (2.5 - 4.2)	0.46 (0.44 - 0.48)	3.1 (2.9 - 3.4)	3.0 (2.9 - 3.1)	0.11 (0.06 - 0.17)
8	45	5.0 (4.7 - 5.3)	1.0 (0.6 - 1.4)	0.34 (0.31 - 0.38)	7.0 (5.7 - 8.3)	2.5 (1.9 - 3.2)	0.51 (0.47 - 0.58)	1.1	1.5	0.51
9	21	3.6 (2.7 - 4.5)	1.8 (1.6 - 2.0)	0.75 (0.64 - 0.85)	8.9 (7.4 - 10.3)	4.2 (3.9 - 4.6)	0.77 (0.68 - 0.85)	5.4 (4.5 - 6.3)	3.2 (2.6 - 3.7)	0.24 (0.17 - 0.32)

10	10	5.2 (4.9 - 5.5)	2.6 (2.3 - 2.8)	0.50 (0.41 - 0.59)	8.9 (8.3 - 9.5)	3.8 (3.7 - 4.0)	0.62 (0.51 - 0.73)	3.5 (3.1 - 3.9)	2.5 (2.4 - 2.6)	0.47 (0.32 - 0.62)
11	24	6.0 (4.1 - 7.9)	2.5 (1.8 - 3.3)	0.46 (0.42 - 0.49)	13.1	4.3	0.82	4.0 (2.5 - 6.8)	4.0 (2.8 - 6.0)	0.23 (0.04 - 0.44)
12	35	18.1 (16.4 - 19.8)	5.8 (5.6 - 6.1)	0.77 (0.76 - 0.79)	11.6 (9.1 - 14.1)	6.3 (5.4 - 7.1)	0.70 (0.68 - 0.72)	5.3 (4.7 - 6.0)	5.5 (5.3 - 5.8)	0.25
13	41	11.6 (6.9 - 16.4)	3.5 (2.5 - 4.4)	0.55 (0.51 - 0.58)	8.9 (8.3 - 9.5)	4.6 (3.0 - 5.6)	0.16 (0 - 0.48)	5.9 (3.3 - 7.6)	5.2 (4.1 - 5.7)	0.12 (0 - 0.30)

1
2 Table 4. Concentrations of CH₃I, CH₂I₂ and the sum of TChl *a* averaged over different depths at every CTD station (1 – 13), as well as the
3 mixed layer depth. If a range is not given, only one measurement point exists. Bold numbers indicate the depth of maximum concentrations at
4 this station.

<i>z_{ML}</i> [m]	0 – 30 m		30 – 60 m		60 – 100 m		
	Concentrations [pmol L ⁻¹]		TChl <i>a</i> [µg L ⁻¹]	Concentrations [pmol L ⁻¹]		TChl <i>a</i> [µg L ⁻¹]	
	CH ₃ I	CH ₂ I ₂		CH ₃ I	CH ₂ I ₂	CH ₃ I	CH ₂ I ₂

1	34	2.7 (2.1 - 3.4)	4.5 (1.2 - 6.8)	0.60 (0.52 - 0.69)	2.5 (1.8 - 3.2)	9.9 (3.9 - 16.0)	0.59 (0.53 - 0.65)	0.2	1.7	---
2	16	2.8 (0.4 - 5.2)	4.8 (1.7 - 8.0)	0.92 (0.76 - 1.07)	3.1 (2.7 - 3.6)	12.2 (11.5 - 12.9)	0.86 (0.74 - 0.97)	0.6 (0.1 - 1.3)	2.0 (0.7 - 4.3)	0.20 (0.10 - 0.30)
3	37	8.5 (8.4 - 8.5)	4.1 (1.7 - 6.4)	0.80 (0.75 - 0.86)	2.6 (1.0 - 3.5)	4.6 (4.3 - 4.9)	0.65 (0.51 - 0.80)	0.7 (0.4 - 1.1)	3.3 (2.3 - 4.4)	0.18
4	14	6.1 (5.5 - 6.6)	7.0	0.56 (0.26 - 0.86)	4.6 (4.6 - 4.7)	2.3 (2.2 - 2.4)	0.80 (0.79 - 0.81)	0.8 (0.7 - 0.9)	1.0 (0.7 - 1.3)	0.19 (0.13 - 0.26)
5	49	5.4	0.6 (0.5 - 0.7)	0.34 (0.28 - 0.39)	4.5	4.9	0.58	2.4 (1.9 - 3.0)	10.5 (7.1 - 13.8)	0.39 (0.24 - 0.53)
6	12	10.4 (8.0 - 12.8)	6.9 (1.8 - 12.0)	0.99	1.6 (1.5 - 1.7)	4.0 (3.1 - 4.8)	0.30 (0.17 - 0.43)	1.4 (1.0 - 1.7)	2.4 (1.7 - 3.1)	0.10 (0.04 - 0.17)
7	---	4.1 (3.4 - 4.8)	2.3 (1.2 - 3.4)	0.71 (0.65 - 0.76)	1.3 (1.2 - 1.3)	4.7 (3.3 - 6.1)	0.46 (0.44 - 0.48)	0.9 (0.6 - 1.2)	2.0 (1.5 - 2.7)	0.11 (0.06 - 0.17)
8	45	0.2 (0.1 - 0.4)	0.3 (0.3 - 0.3)	0.34 (0.31 - 0.38)	4.7 (3.0 - 7.0)	1.2 (0.5 - 1.9)	0.51 (0.47 - 0.58)	0.0	2.4	0.51
9	21	4.4 (4.1 - 4.8)	1.3 (1.2 - 1.5)	0.75 (0.64 - 0.85)	5.3 (3.4 - 7.3)	6.2 (4.5 - 8.0)	0.77 (0.68 - 0.85)	1.3 (1.3 - 1.3)	2.9 (2.3 - 3.6)	0.24 (0.17 - 0.32)

10	10	4.5 (3.6 - 5.5)	0.5 (0.4 - 0.6)	0.50 (0.41 - 0.59)	4.9 (4.2 - 5.7)	1.3 (0.9 - 1.7)	0.62 (0.51 - 0.73)	0.8 (0.7 - 0.9)	3.4 (2.6 - 4.1)	0.47 (0.32 - 0.62)
11	24	3.8 (2.9 - 4.6)	0.4	0.46 (0.42 - 0.49)	4.4	2.3	0.82	1.7 (1.0 - 2.3)	1.7 (0.6 - 3.2)	0.23 (0.04 - 0.44)
12	35	7.0 (6.8 - 7.1)	1.2 (0.3 - 2.2)	0.77 (0.76 - 0.79)	2.7	4.1 (3.8 - 4.3)	0.70 (0.68 - 0.72)	2.0	2.7 (1.6 - 3.8)	0.25
13	41	5.1 (4.3 - 5.9)	1.5 (0.8 - 2.1)	0.55 (0.51 - 0.58)	3.8 (2.0 - 5.6)	5.9 (3.9 - 7.4)	0.16 (0 - 0.48)	1.0 (0.1 - 2.0)	3.4 (1.0 - 4.8)	0.12 (0 - 0.30)

1

2 Table 5. Diapycnal and sea-to-air fluxes at every CTD station for the four halocarbons. Positive fluxes in bold provide the mixed layer with
3 the corresponding halocarbon, while negative fluxes indicate losses from the mixed layer.

CTD station	CHBr ₃		CH ₂ Br ₂		CH ₃ I		CH ₂ I ₂	
	Diapycnal flux	Sea-to-air flux	Diapycnal flux	Sea-to-air flux	Diapycnal flux	Sea-to-air flux	Diapycnal flux	Sea-to-air flux
	[pmol m ⁻² h ⁻¹]	[pmol m ⁻² h ⁻¹]	[pmol m ⁻² h ⁻¹]	[pmol m ⁻² h ⁻¹]	[pmol m ⁻² h ⁻¹]	[pmol m ⁻² h ⁻¹]	[pmol m ⁻² h ⁻¹]	[pmol m ⁻² h ⁻¹]
1	14	14	8	-27	5	-119	39	-64

2	-125	-3651	-8	-689	-13	-44	29	-199
3	0	-184	1	-195	-6	-703	7	-129
4	8	-241	4	-265	-1	-671	3	---
5	-3	-893	4	-275	-2	---	9	-45
6	5	-590	7	-185	-13	-988	27	-121
7	---	---	---	---	---	---	---	---
8	-2	-110	-0	-25	-1	-4	0	-22
9	3	-57	1	-64	1	-337	3	-88
10	2	-45	-2	-83	-6	-300	-1	-30
11	4	-248	1	-136	1	-316	0	-24
12	-4	-1208	-1	-357	-2	-583	-0	-20
13	1	-837	0	-231	-3	-446	-4	-54

1
 2 Table 6. Total mixed layer budget of each halocarbon, potential sinks and sources (box size $1 \times 1 \times z_{ML}$ m³). The upper four rows indicate
 3 cases where diapycnal fluxes act as sources, while the lower four rows summarize the budget for the cases where the diapycnal fluxes were
 4 sinks for the mixed layer budget. “Other sinks” is halogen substitution for CH₃I and photolysis in case of CH₂I₂. The negative numbers
 5 indicate sinks for the budget.

	Compound	z_{ML}	Total ML budget	Air-sea fluxes (S_{as})	Diapycnal fluxes (F_{dia})	Other sinks (S_{ch})	Total after 1 h	Difference
Unit		[m]	[pmol]	[pmol h⁻¹]	[pmol h⁻¹]	[pmol h⁻¹]	[pmol]	[pmol]
	CHBr ₃	24	157543	-274	5		157274	-269
Diapycnal fluxes as source	CH ₂ Br ₂	29	90058	-172	3		89889	-169
	CH ₃ I	26	75263	-257	2	0	75004	-255
	CH ₂ I ₂	28	63947	-78	13	-8317	55565	-8382
	CHBr ₃	36	417098	-1186	-30		415882	-1216
Diapycnal fluxes as sink	CH ₂ Br ₂	27	99604	-236	-2		99366	-238
	CH ₃ I	29	137560	-420	-5	0	137135	-425

CH ₂ I ₂	29	106587	-35	-2	-4977	101573	-5014
--------------------------------	----	--------	-----	----	-------	--------	--------------

1

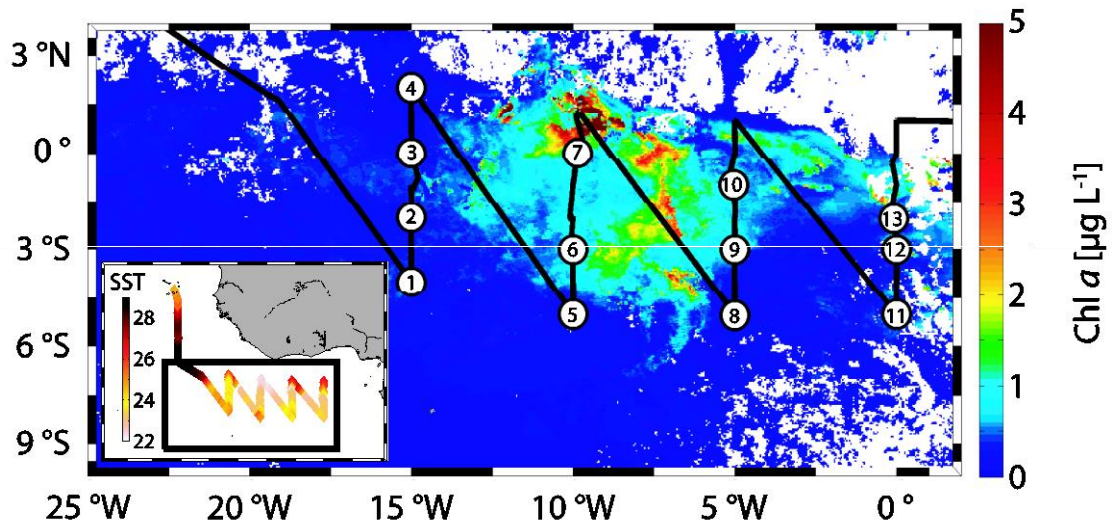
2 Table 7. Theoretical mean production rate of the four halocarbons in the equatorial mixed layer with the standard deviation.

Compound	Production rate [pmol m ⁻³ h ⁻¹]	Standard deviation [pmol m ⁻³ h ⁻¹]	Production rate per TChl <i>a</i> [pmol [μg TChl <i>a</i>] ⁻¹ h ⁻¹]
CHBr ₃	34	65	2.5 x 10 ⁻³
CH ₂ Br ₂	10	12	8.5 x 10 ⁻⁴
CH ₃ I	21	24	2.2 x 10 ⁻³
CH ₂ I ₂	384	318	3.3 x 10 ⁻²

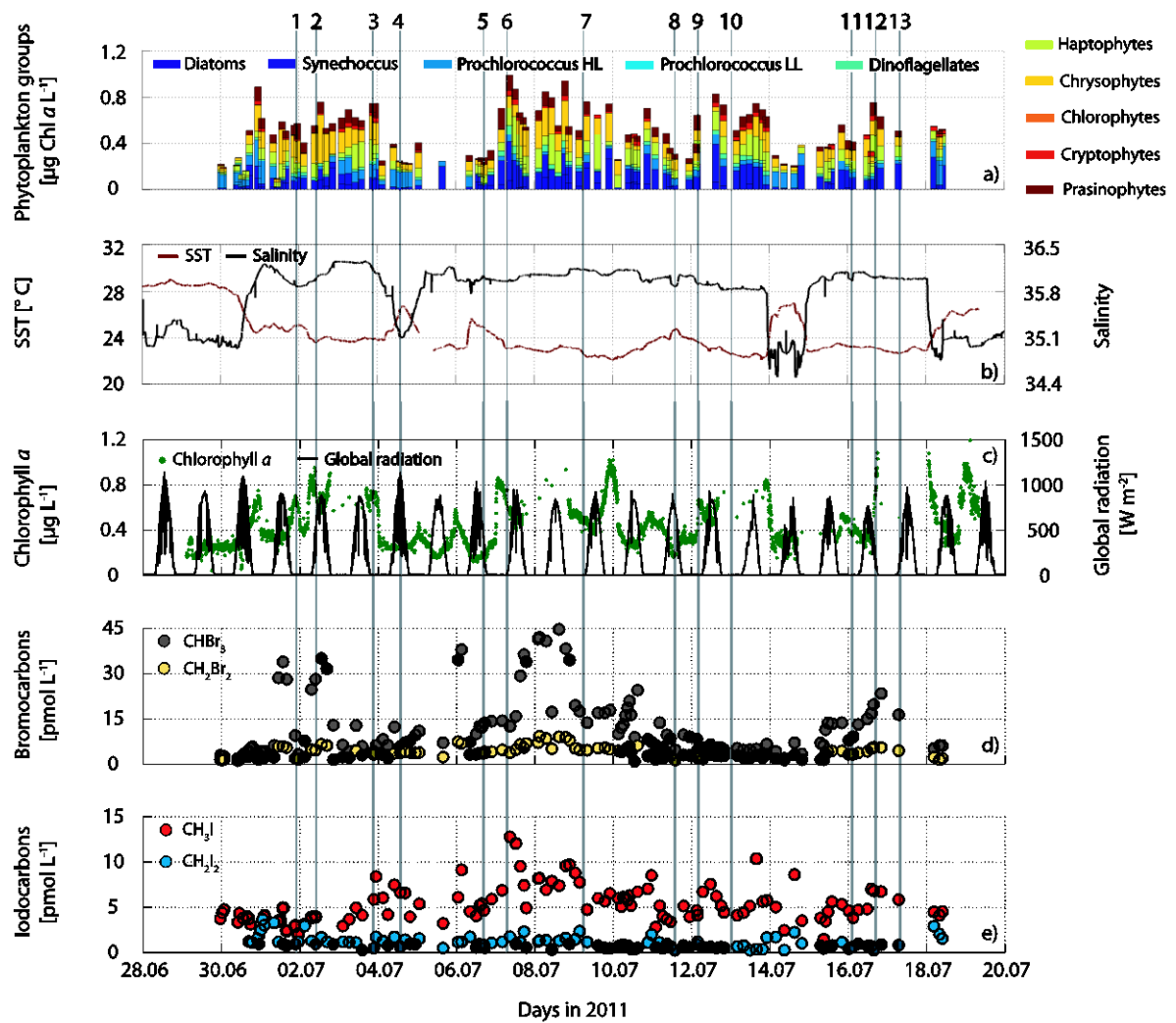
3

4

1 Figures

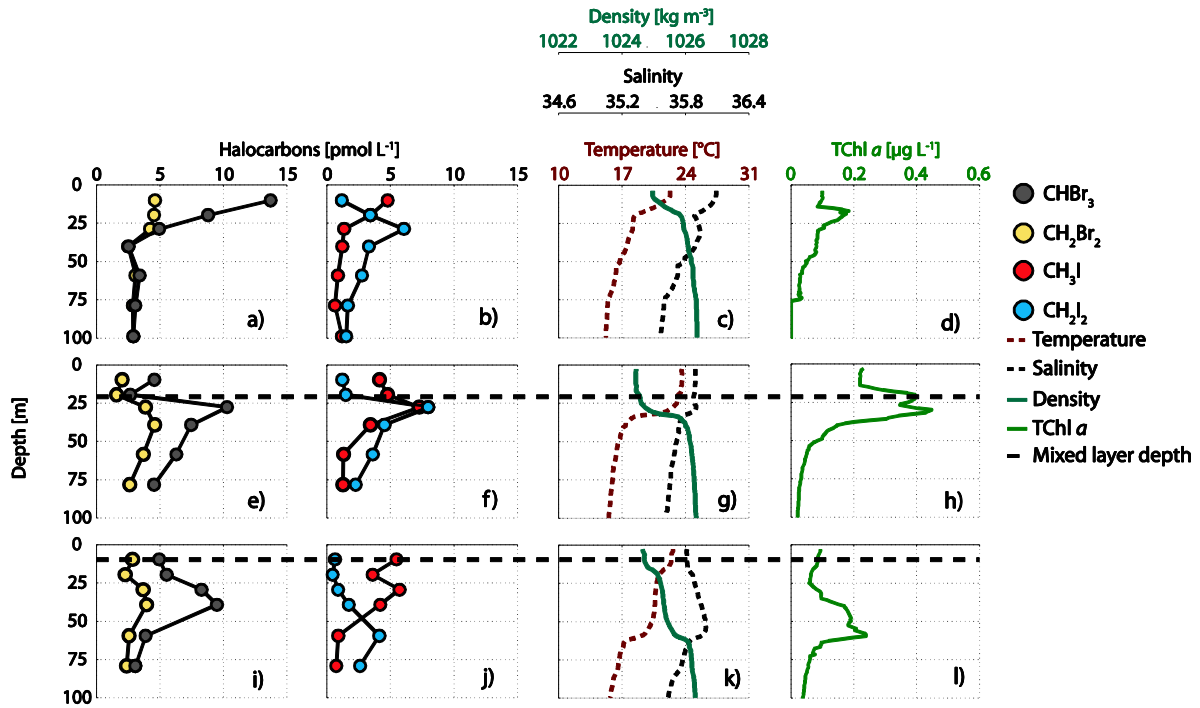


2
3 Figure 1. Cruise track with SST in °C (small box) and the section (large box) were
4 halocarbons were sampled in both the sea surface and during CTD stations (numbered
5 circles), plotted on monthly average Chl *a* for July 2011 derived from mapped level 3 MODIS
6 Aqua Data.



1
 2 Figure 2. a) Species composition (HL – high light, LL – low light), b) SST and salinity during
 3 the cruise, c) TChl a from underway fluorescence sensor measurements and global radiation,
 4 e) CHBr_3 and CH_2Br_2 in surface sea water, and e) CH_3I and CH_2I_2 surface sea water
 5 concentrations. The top numbers mark the CTD stations.

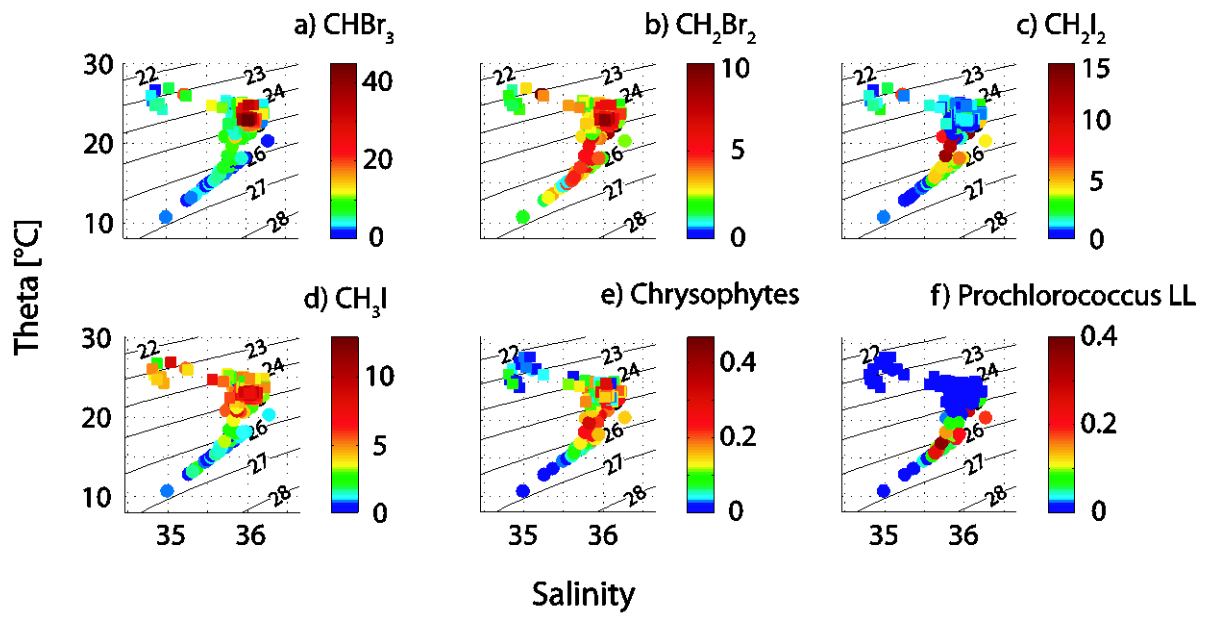
1



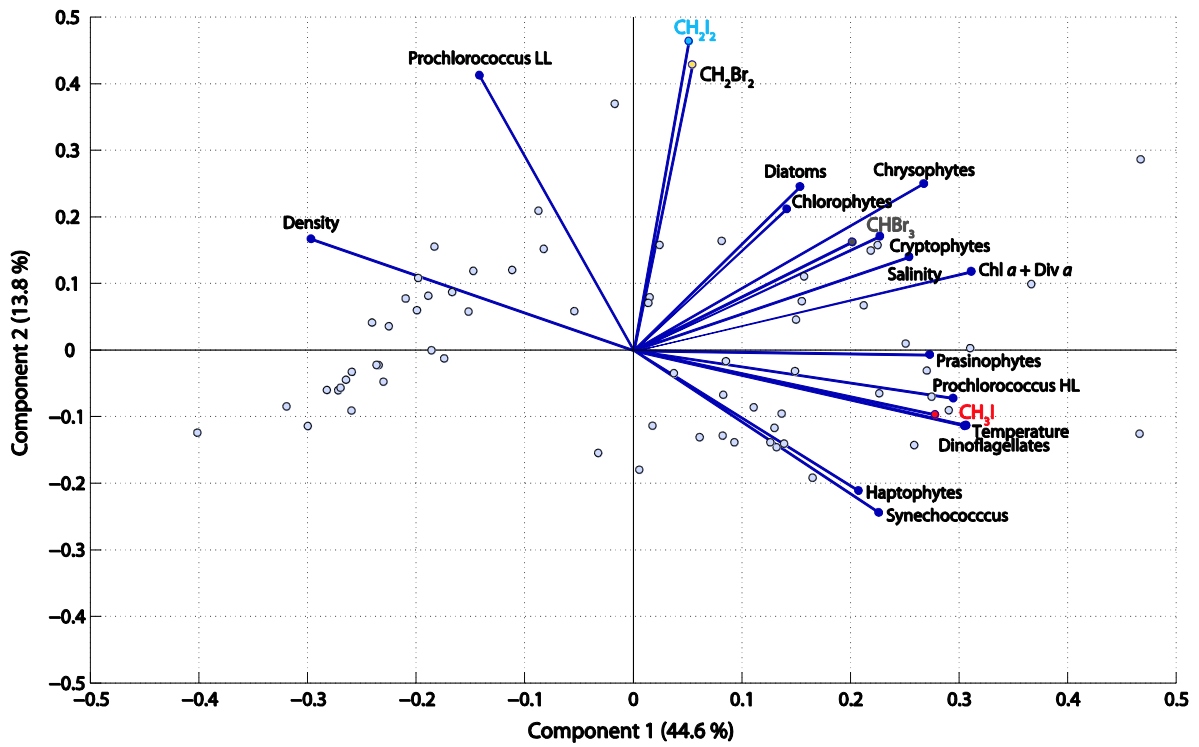
2

3 Figure 3. Selected CTD profiles (top – down: profiles 7, 9 and 10, see Figure 1 for the
 4 location) of CHBr₃, CH₂Br₂, CH₃I, and CH₂I₂ in a – b), e – f), and i – j), along with
 5 temperature, salinity, and density (c, g and k), as well as TChl *a* in d), h), and l), and the
 6 mixed layer depth as black dashed line at the same stations.

7

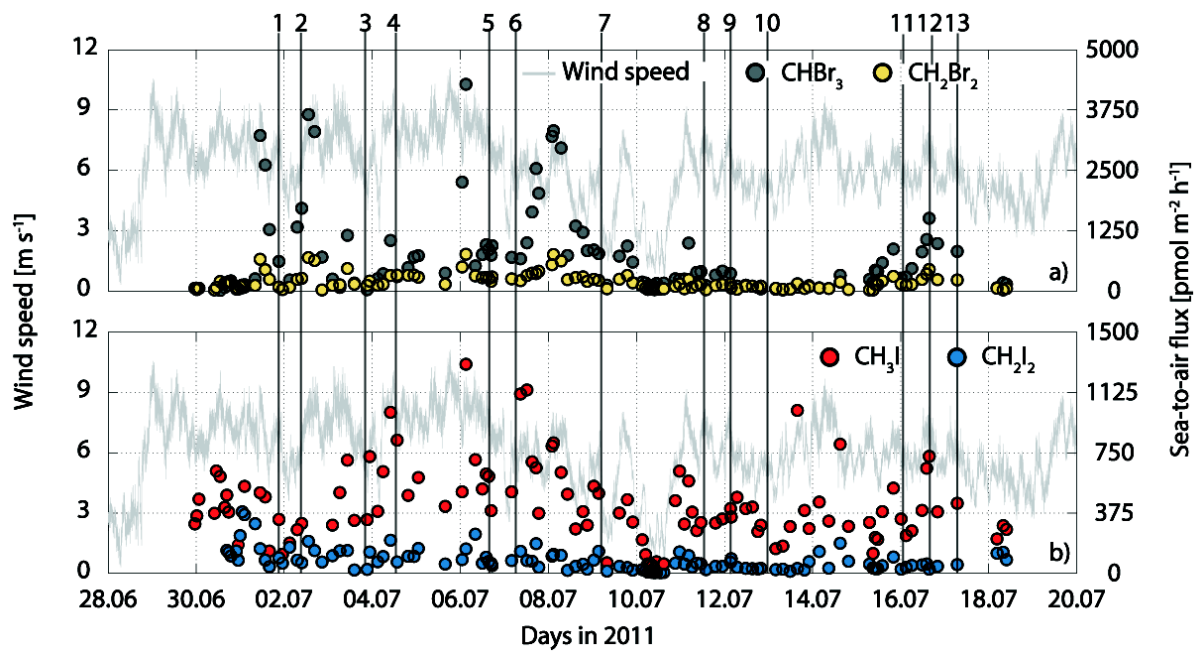


1
 2 Figure 4. a – d) Temperature-Salinity (T-S) plots for halocarbons (in pmol L^{-1}) and e – f)
 3 phytoplankton species (in $\mu\text{g Chl } a \text{ L}^{-1}$). Square markers indicate surface values of
 4 halocarbons from underway measurements, circles are depth measurements from CTD
 5 profile, and the lines indicate the potential density – 1000.
 6



1
 2 Figure 5. Principal component analysis (PCA) of halocarbon and phytoplankton species
 3 composition data, as well as temperature, salinity, and density for the 13 CTD stations during
 4 MSM18/3.

5



1
2
3
4
5

Figure 6. Wind speed during the cruise and sea-to-air fluxes calculated with sea surface water concentrations and mean atmospheric halocarbon data a) CHBr_3 and CH_2Br_2 and b) CH_3I and CH_2I_2 . Numbers on the top indicate CTD stations.

1 References

- 2
- 3 Abrahamsson, K., Bertilsson, S., Chierici, M., Fransson, A., Froneman, P. W., Loren, A., and
4 Pakhomov, E. A.: Variations of biochemical parameters along a transect in the southern
5 ocean, with special emphasis on volatile halogenated organic compounds, *Deep-Sea Res. Part*
6 *II-Top. Stud. Oceanogr.*, 51, 2745-2756, 10.1016/j.dsr2.2004.09.004, 2004a.
- 7 Abrahamsson, K., Lorén, A., Wulff, A., and Wangberg, S. A.: Air-sea exchange of
8 halocarbons: The influence of diurnal and regional variations and distribution of pigments,
9 *Deep-Sea Res. Part II-Top. Stud. Oceanogr.*, 51, 2789-2805, 10.1016/j.dsr2.2004.09.005,
10 2004b.
- 11 Amachi, S., Kamagata, Y., Kanagawa, T., and Muramatsu, Y.: Bacteria mediate methylation
12 of iodine in marine and terrestrial environments, *Applied and Environmental Microbiology*,
13 67, 2718-2722, 10.1128/aem.67.6.2718-2722.2001, 2001.
- 14 Amachi, S., Muramatsu, Y., Akiyama, Y., Miyazaki, K., Yoshiki, S., Hanada, S., Kamagata,
15 Y., Ban-nai, T., Shinoyama, H., and Fujii, T.: Isolation of iodide-oxidizing bacteria from
16 iodide-rich natural gas brines and seawaters, *Microb. Ecol.*, 49, 547-557, 10.1007/s00248-
17 004-0056-0, 2005.
- 18 Amachi, S.: Microbial contribution to global iodine cycling: Volatilization, accumulation,
19 reduction, oxidation, and sorption of iodine, *Microbes Environ.*, 23, 269-276,
20 10.1264/jsme2.ME08548, 2008.
- 21 Aschmann, J., Sinnhuber, B. M., Chipperfield, M. P., and Hossaini, R.: Impact of deep
22 convection and dehydration on bromine loading in the upper troposphere and lower
23 stratosphere, *Atmos. Chem. Phys.*, 11, 2671-2687, 10.5194/acp-11-2671-2011, 2011.
- 24 Barlow, R. G., Cummings, D. G., and Gibb, S. W.: Improved resolution of mono- and divinyl
25 chlorophylls a and b and zeaxanthin and lutein in phytoplankton extracts using reverse phase
26 c-8 hplc, *Marine Ecology Progress Series*, 161, 303-307, 10.3354/meps161303, 1997.
- 27 Bracher A., Taylor B.B., Taylor M., Dinter T., Röttgers R., Steinmetz F. (2015) Using
28 empirical orthogonal functions derived from remote sensing reflectance for the prediction of
29 concentrations of phytoplankton pigments. *Ocean Science* 11: 139-158.
- 30 Brownell, D. K., Moore, R. M., and Cullen, J. J.: Production of methyl halides by
31 prochlorococcus and synechococcus, *Glob. Biogeochem. Cycles*, 24, 10.1029/2009gb003671,
32 2010.
- 33 Carpenter, L. J. and Liss, P. S.: On temperate sources of bromoform and other reactive
34 organic bromine gases, *J. Geophys. Res.-Atmos.*, 105, 20539-20547, 10.1029/2000JD900242.
- 35 Carpenter, L. J., Malin, G., Liss, P. S., and Kupper, F. C.: Novel biogenic iodine-containing
36 trihalomethanes and other short-lived halocarbons in the coastal east atlantic, *Glob.*
37 *Biogeochem. Cycles*, 14, 1191-1204, 10.1029/2000GB001257, 2000.
- 38 Carpenter, L. J., Wevill, D. J., Palmer, C. J., and Michels, J.: Depth profiles of volatile iodine
39 and bromine-containing halocarbons in coastal antarctic waters, *Mar. Chem.*, 103, 227-236,
40 10.1016/j.marchem.2006.08.003, 2007.

- 1 Carpenter, L. J., Jones, C. E., Dunk, R. M., Hornsby, K. E., and Woeltjen, J.: Air-sea fluxes of
2 biogenic bromine from the tropical and north atlantic ocean, *Atmos. Chem. Phys.*, 9, 1805-
3 1816, 10.5194/acp-9-1805-2009, 2009.
- 4 Claustre, H., and Marty, J. C.: Specific phytoplankton biomasses and their relation to primary
5 production in the tropical north-atlantic, *Deep-Sea Res. Part I-Oceanogr. Res. Pap.*, 42, 1475-
6 1493, 10.1016/0967-0637(95)00053-9, 1995.
- 7 Elliott, S., and Rowland, F. S.: Nucleophilic substitution rates and solubilities for methyl
8 halides in seawater, *Geophys. Res. Lett.*, 20, 1043-1046, 10.1029/93gl01081, 1993.
- 9 Elliott, S., and Rowland, F. S.: Methyl halide hydrolysis rates in natural waters, *J. Atmos.*
10 *Chem.*, 20, 229-236, 10.1007/bf00694495, 1995.
- 11 Fujiki, T., Matsumoto, K., Watanabe, S., Hosaka, T., and Saino, T.: Phytoplankton
12 productivity in the western subarctic gyre of the north pacific in early summer 2006, *J.*
13 *Oceanogr.*, 67, 295-303, 10.1007/s10872-011-0028-1, 2011.
- 14 Fuse, H., Inoue, H., Murakami, K., Takimura, O., and Yamaoka, Y.: Production of free and
15 organic iodine by *roseovarius* spp, *FEMS Microbiology Letters*, 229, 189-194,
16 10.1016/s0378-1097(03)00839-5, 2003.
- 17 Geen, C. E.: Selected marine sources and sinks of bromoform and other low molecular weight
18 organobromines, PhD, Dalhousie University, Halifax, Halifax, Nova Scotia, 1992.
- 19 Goodwin, K. D., Schaefer, J. K., and Oremland, R. S.: Bacterial oxidation of dibromomethane
20 and methyl bromide in natural waters and enrichment cultures, *Applied and Environmental*
21 *Microbiology*, 64, 4629-4636, 1998.
- 22 Grodsky, S. A., Carton, J. A., and McClain, C. R.: Variability of upwelling and chlorophyll in
23 the equatorial atlantic, *Geophys. Res. Lett.*, 35, L03610, 10.1029/2007gl032466, 2008.
- 24 Happell, J. D., and Wallace, D. W. R.: Methyl iodide in the greenland/norwegian seas and the
25 tropical atlantic ocean: Evidence for photochemical production, *Geophys. Res. Lett.*, 23,
26 2105-2108, 10.1029/96gl01764, 1996.
- 27 Hense, I., and Quack, B.: Modelling the vertical distribution of bromoform in the upper water
28 column of the tropical atlantic ocean, *Biogeosciences*, 6, 535-544, 10.5194/bg-6-535-2009,
29 2009.
- 30 Hepach, H., Quack, B., Ziska, F., Fuhlbrügge, S., Atlas, E. L., Krüger, K., Peeken, I., and
31 Wallace, D. W. R.: Drivers of diel and regional variations of halocarbon emissions from the
32 tropical north east atlantic, *Atmos. Chem. Phys.*, 14, 1255-1275, 10.5194/acp-14-1255-2014,
33 2014.
- 34 Hopkins, F. E., Kimmance, S. A., Stephens, J. A., Bellerby, R. G. J., Brussaard, C. P. D.,
35 Czerny, J., Schulz, K. G., and Archer, S. D.: Response of halocarbons to ocean acidification
36 in the arctic, *Biogeosciences*, 10, 2331-2345, 10.5194/bg-10-2331-2013, 2013.
- 37 Hossaini, R., Chipperfield, M. P., Monge-Sanz, B. M., Richards, N. A. D., Atlas, E., and
38 Blake, D. R.: Bromoform and dibromomethane in the tropics: A 3-d model study of chemistry
39 and transport, *Atmos. Chem. Phys.*, 10, 719-735, 10.5194/acp-10-719-2010, 2010.
- 40 Hossaini, R., Chipperfield, M. P., Feng, W., Breider, T. J., Atlas, E., Montzka, S. A., Miller,
41 B. R., Moore, F., and Elkins, J.: The contribution of natural and anthropogenic very short-
42 lived species to stratospheric bromine, *Atmos. Chem. Phys.*, 12, 371-380, 10.5194/acp-12-
43 371-2012, 2012.

- 1 Hughes, C., Chuck, A. L., Rossetti, H., Mann, P. J., Turner, S. M., Clarke, A., Chance, R.,
2 and Liss, P. S.: Seasonal cycle of seawater bromoform and dibromomethane concentrations in
3 a coastal bay on the western antarctic peninsula, *Glob. Biogeochem. Cycles*, 23, Gb2024,
4 10.1029/2008gb003268, 2009.
- 5 Hughes, C., Franklin, D. J., and Malin, G.: Iodomethane production by two important marine
6 cyanobacteria: *Prochlorococcus marinus* (ccmp 2389) and *synechococcus* sp (ccmp 2370),
7 *Mar. Chem.*, 125, 19-25, 10.1016/j.marchem.2011.01.007, 2011.
- 8 Hughes, C., Johnson, M., Utting, R., Turner, S., Malin, G., Clarke, A., and Liss, P. S.:
9 Microbial control of bromocarbon concentrations in coastal waters of the western antarctic
10 peninsula, *Mar. Chem.*, 151, 35-46, 10.1016/j.marchem.2013.01.007, 2013.
- 11 Hummels, R., Dengler, M., and Bourles, B.: Seasonal and regional variability of upper ocean
12 diapycnal heat flux in the atlantic cold tongue, *Prog. Oceanogr.*, 111, 52-74,
13 10.1016/j.pocean.2012.11.001, 2013.
- 14 Itoh, N., Tsujita, M., Ando, T., Hisatomi, G., and Higashi, T.: Formation and emission of
15 monohalomethanes from marine algae, *Phytochemistry*, 45, 67-73, 10.1016/s0031-
16 9422(96)00786-8, 1997.
- 17 Jin, Z. H., Charlock, T. P., Rutledge, K., Starnes, K., and Wang, Y. J.: Analytical solution of
18 radiative transfer in the coupled atmosphere-ocean system with a rough surface, *Appl. Optics*,
19 45, 7443-7455, 10.1364/ao.45.007443, 2006.
- 20 Johnson, Z. I., Zinser, E. R., Coe, A., McNulty, N. P., Woodward, E. M. S., and Chisholm, S.
21 W.: Niche partitioning among *prochlorococcus* ecotypes along ocean-scale environmental
22 gradients, *Science*, 311, 1737-1740, 10.1126/science.1118052, 2006.
- 23 Jones, C. E., and Carpenter, L. J.: Solar photolysis of ch_2i_2 , ch_2ici , and ch_2ibr in water,
24 saltwater, and seawater, *Environ. Sci. Technol.*, 39, 6130-6137, 10.1021/es050563g, 2005.
- 25 Jones, C. E., and Carpenter, L. J.: Chemical destruction of $ch_3ic_2h_5i$, c_2h_5i , $1-c_3h_7i$, and $2-$
26 c_3h_7i in saltwater, *Geophys. Res. Lett.*, 34, L13804, 10.1029/2007gl029775, 2007.
- 27 Jones, C. E., Hornsby, K. E., Sommariva, R., Dunk, R. M., Von Glasow, R., McFiggans, G.,
28 and Carpenter, L. J.: Quantifying the contribution of marine organic gases to atmospheric
29 iodine, *Geophys. Res. Lett.*, 37, L18804, 10.1029/2010gl043990, 2010.
- 30 Jouanno, J., Marin, F., du Penhoat, Y., Sheinbaum, J., and Molines, J. M.: Seasonal heat
31 balance in the upper 100 m of the equatorial atlantic ocean, *J. Geophys. Res.-Oceans*, 116,
32 10.1029/2010jc006912, 2011.
- 33 Kara, A. B., Rochford, P. A., and Hurlburt, H. E.: An optimal definition for ocean mixed
34 layer depth, *J. Geophys. Res.-Oceans*, 105, 16803-16821, 10.1029/2000jc900072, 2000.
- 35 Karlsson, A., Auer, N., Schulz-Bull, D., and Abrahamsson, K.: Cyanobacterial blooms in the
36 baltic - a source of halocarbons, *Mar. Chem.*, 110, 129-139, 10.1016/j.marchem.2008.04.010,
37 2008.
- 38 Kirkham, A. R., Jardillier, L. E., Tiganescu, A., Pearman, J., Zubkov, M. V., and Scanlan, D.
39 J.: Basin-scale distribution patterns of photosynthetic picoeukaryotes along an atlantic
40 meridional transect, *Environ. Microbiol.*, 13, 975-990, 10.1111/j.1462-2920.2010.02403.x,
41 2011.
- 42 Klick, S., and Abrahamsson, K.: Biogenic volatile iodated hydrocarbons in the ocean, *J.*
43 *Geophys. Res.-Oceans*, 97, 12683-12687, 10.1029/92jc00948, 1992.

- 1 Kolber, Z., and Falkowski, P. G.: Use of active fluorescence to estimate phytoplankton
2 photosynthesis in-situ, *Limnol. Oceanogr.*, 38, 1646-1665, 10.4319/lo.1993.38.8.1646, 1993.
- 3 Kurihara, M. K., Kimura, M., Iwamoto, Y., Narita, Y., Ooki, A., Eum, Y. J., Tsuda, A.,
4 Suzuki, K., Tani, Y., Yokouchi, Y., Uematsu, M., and Hashimoto, S.: Distributions of short-
5 lived iodocarbons and biogenic trace gases in the open ocean and atmosphere in the western
6 north pacific, *Mar. Chem.*, 118, 156-170, 10.1016/j.marchem.2009.12.001, 2010.
- 7 Laturnus, F.: Marine macroalgae in polar regions as natural sources for volatile
8 organohalogenes, *Environ. Sci. Pollut. Res.*, 8, 103-108, 10.1007/bf02987302, 2001.
- 9 Lin, C. Y., and Manley, S. L.: Bromoform production from seawater treated with
10 bromoperoxidase, *Limnol. Oceanogr.*, 57, 1857-1866, 10.4319/lo.2012.57.06.1857, 2012.
- 11 Liu, Y. N., Yvon-Lewis, S. A., Hu, L., Salisbury, J. E., and O'Hern, J. E.: Chbr(3), ch(2)br(2),
12 and chlbr(2) in u.S. Coastal waters during the gulf of mexico and east coast carbon cruise, *J.*
13 *Geophys. Res.-Oceans*, 116, C10004, 10.1029/2010jc006729, 2011.
- 14 Liu, Y. N., Yvon-Lewis, S. A., Thornton, D. C. O., Campbell, L., and Bianchi, T. S.: Spatial
15 distribution of brominated very short-lived substances in the eastern pacific, *J. Geophys. Res.-*
16 *Oceans*, 118, 2318-2328, 10.1002/jgrc.20183, 2013a.
- 17 Liu, Y. N., Yvon-Lewis, S. A., Thornton, D. C. O., Butler, J. H., Bianchi, T. S., Cambell, L.,
18 Hu, L., and Smith, R. W.: Spatial and temporal distributions of bromoform and
19 dibromomethane in the atlantic ocean and their relationship with photosynthetic biomass, *J.*
20 *Geophys. Res.-Oceans*, 118, 3950-3965, 10.1002/jgrc.20299, 2013b.
- 21 Liu, Y. N., Thornton, D. C. O., Bianchi, T. S., Arnold, W. A., Shields, M. R., Chen, J., and
22 Yvon-Lewis, S. A.: Dissolved organic matter composition drives the marine production of
23 brominated very short-lived substances, *Environ. Sci. Technol.*, 49, 3366-3374,
24 10.1021/es505464k, 2015.
- 25 Mabey, W., and Mill, T.: Critical review of hydrolysis of organic compounds in water under
26 environmental conditions, *J. Phys. Chem. Ref. Data*, 7, 383-415, 10.1063/1.555572, 1978.
- 27 Mackey, M. D., Mackey, D. J., Higgins, H. W., and Wright, S. W.: Chemtax - a program for
28 estimating class abundances from chemical markers: Application to hplc measurements of
29 phytoplankton, *Mar. Ecol.-Prog. Ser.*, 144, 265-283, 10.3354/meps144265, 1996.
- 30 Manley, S. L., and Dastoor, M. N.: Methyl-iodide (ch₃i) production by kelp and associated
31 microbes, *Mar. Biol.*, 98, 477-482, 10.1007/BF00391538, 1988.
- 32 Manley, S. L., and de la Cuesta, J. L.: Methyl iodide production from marine phytoplankton
33 cultures, *Limnol. Oceanogr.*, 42, 142-147, 10.4319/lo.1997.42.1.0142, 1997.
- 34 Martino, M., Liss, P. S., and Plane, J. M. C.: The photolysis of dihalomethanes in surface
35 seawater, *Environ. Sci. Technol.*, 39, 7097-7101, 10.1021/es048718s, 2005.
- 36 Martino, M., Liss, P. S., and Plane, J. M. C.: Wavelength-dependence of the photolysis of
37 diiodomethane in seawater, *Geophys. Res. Lett.*, 33, L06606, 10.1029/2005gl025424, 2006.
- 38 Martino, M., Mills, G. P., Woeltjen, J., and Liss, P. S.: A new source of volatile organoiodine
39 compounds in surface seawater, *Geophys. Res. Lett.*, 36, L01609, 10.1029/2008gl036334,
40 2009.
- 41 Molinari, R. L.: Observations of eastwad currents in the tropical south-atlantic ocean - 1978 -
42 1980, *J. Geophys. Res.-Oceans and Atmospheres*, 87, 9707-9714,
43 10.1029/JC087iC12p09707, 1982.

- 1 Moore, R. M., and Tokarczyk, R.: Volatile biogenic halocarbons in the northwest atlantic,
2 *Glob. Biogeochem. Cycles*, 7, 195-210, 10.1029/92GB02653, 1993.
- 3 Moore, R. M., and Zafiriou, O. C.: Photochemical production of methyl-iodide in seawater, *J.*
4 *Geophys. Res.-Atmos.*, 99, 16415-16420, 10.1029/94jd00786, 1994.
- 5 Moore, R. M., Geen, C. E., and Tait, V. K.: Determination of henry law constants for a suite
6 of naturally-occurring halogenated methanes in seawater, *Chemosphere*, 30, 1183-1191,
7 10.1016/0045-6535(95)00009-w, 1995a.
- 8 Moore, R. M., Tokarczyk, R., Tait, V. K., Poulin, M., and Geen, C. E.: Marine phytoplankton
9 as a natural source of volatile organohalogenes, in: *Naturally-produced organohalogenes*, edited
10 by: Grimvall, A., and deLeer, E. W. B., Kluwer Academic Publishers, Dordrecht, 283-294,
11 1995b.
- 12 Moore, R. M., Webb, M., Tokarczyk, R., and Wever, R.: Bromoperoxidase and
13 iodoperoxidase enzymes and production of halogenated methanes in marine diatom cultures,
14 *J. Geophys. Res.-Oceans*, 101, 20899-20908, 10.1029/96jc01248, 1996.
- 15 Moore, R. M., and Groszko, W.: Methyl iodide distribution in the ocean and fluxes to the
16 atmosphere, *J. Geophys. Res.-Oceans*, 104, 11163-11171, 10.1029/1998jc900073, 1999.
- 17 Nightingale, P. D., Malin, G., and Liss, P. S.: Production of chloroform and other low-
18 molecular-weight halocarbons by some species of macroalgae, *Limnol. Oceanogr.*, 40, 680-
19 689, 10.4319/l0.1995.40.4.0680, 1995.
- 20 Nightingale, P. D., Malin, G., Law, C. S., Watson, A. J., Liss, P. S., Liddicoat, M. I., Boutin,
21 J., and Upstill-Goddard, R. C.: In situ evaluation of air-sea gas exchange parameterizations
22 using novel conservative and volatile tracers, *Glob. Biogeochem. Cycles*, 14, 373-387,
23 10.1029/1999gb900091, 2000.
- 24 Orlikowska, A., and Schulz-Bull, D. E.: Seasonal variations of volatile organic compounds in
25 the coastal baltic sea, *Environ. Chem.*, 6, 495-507, 10.1071/en09107, 2009.
- 26 Osborn, T. R.: Estimates of the local rate of vertical diffusion from dissipation measurements,
27 *J. Phys. Oceanogr.*, 10, 83-89, 10.1175/1520-0485(1980)010<0083:eotlro>2.0.co;2, 1980.
- 28 Penkett, S. A., Jones, B. M. R., Rycroft, M. J., and Simmons, D. A.: An interhemispheric
29 comparison of the concentrations of bromine compounds in the atmosphere, *Nature*, 318, 550-
30 553, 10.1038/318550a0, 1985.
- 31 Philander, S. G. H., and Pacanowski, R. C.: A model of the seasonal cycle in the tropical
32 atlantic ocean, *J. Geophys. Res.-Oceans*, 91, 14192-14206, 10.1029/JC091iC12p14192, 1986.
- 33 Quack, B., and Wallace, D. W. R.: Air-sea flux of bromoform: Controls, rates, and
34 implications, *Glob. Biogeochem. Cycles*, 17, 1023, 10.1029/2002gb001890, 2003.
- 35 Quack, B., Atlas, E., Petrick, G., Stroud, V., Schauffler, S., and Wallace, D. W. R.: Oceanic
36 bromoform sources for the tropical atmosphere, *Geophys. Res. Lett.*, 31, L23s05,
37 10.1029/2004gl020597, 2004.
- 38 Quack, B., Atlas, E., Petrick, G., and Wallace, D. W. R.: Bromoform and dibromomethane
39 above the mauritanian upwelling: Atmospheric distributions and oceanic emissions, *J.*
40 *Geophys. Res.-Atmos.*, 112, D09312, 10.1029/2006jd007614, 2007a.
- 41 Quack, B., Peeken, I., Petrick, G., and Nachtigall, K.: Oceanic distribution and sources of
42 bromoform and dibromomethane in the mauritanian upwelling, *J. Geophys. Res.-Oceans*, 112,
43 C10006, 10.1029/2006jc003803, 2007b.

- 1 Raimund, S., Quack, B., Bozec, Y., Vernet, M., Rossi, V., Garcon, V., Morel, Y., and Morin,
2 P.: Sources of short-lived bromocarbons in the iberian upwelling system, *Biogeosciences*, 8,
3 1551-1564, 10.5194/bg-8-1551-2011, 2011.
- 4 Richter, U.: Factors influencing methyl iodide production in the ocean and its flux to the
5 atmosphere, PhD, Mathematisch-Naturwissenschaftliche Fakultät der Christian-Albrechts-
6 Universität zu Kiel, Christian-Albrechts-Universität zu Kiel, Kiel, 117 pp., 2004.
- 7 Richter, U., and Wallace, D. W. R.: Production of methyl iodide in the tropical atlantic ocean,
8 *Geophys. Res. Lett.*, 31, L23s03, 10.1029/2004gl020779, 2004.
- 9 Round, F. E.: The chrysophyta - a reassessment, in: *Chrysophytes: Aspects and problems*,
10 edited by: Kristiansen, J., and Andersen, R. A., Cambridge University Press, Cambridge,
11 1986.
- 12 Saiz-Lopez, A., Plane, J. M. C., Baker, A. R., Carpenter, L. J., von Glasow, R., Martin, J. C.
13 G., McFiggans, G., and Saunders, R. W.: Atmospheric chemistry of iodine, *Chem. Rev.*, 112,
14 1773-1804, 10.1021/cr200029u, 2012.
- 15 Scarratt, M. G., and Moore, R. M.: Production of methyl bromide and methyl chloride in
16 laboratory cultures of marine phytoplankton ii, *Mar. Chem.*, 59, 311-320, 10.1016/s0304-
17 4203(97)00092-3, 1998.
- 18 Scarratt, M. G., and Moore, R. M.: Production of chlorinated hydrocarbons and methyl iodide
19 by the red microalga porphyridium purpureum, *Limnol. Oceanogr.*, 44, 703-707,
20 10.4319/lo.1999.44.3.0703, 1999.
- 21 Schafstall, J., Dengler, M., Brandt, P., and Bange, H: Tidal-induced mixing and diapycnal
22 nutrient fluxes in the mauritanian upwelling region, *J. Geophys. Res.-Oceans*, 115, C10014,
23 10.1029/2009jc005940, 2010.
- 24 Schall, C., Heumann, K. G., and Kirst, G. O.: Biogenic volatile organoiodine and
25 organobromine hydrocarbons in the atlantic ocean from 42 degrees n to 72 degrees s,
26 *Fresenius J. Anal. Chem.*, 359, 298-305, 10.1007/s002160050577, 1997.
- 27 Schauffler, S. M., Atlas, E. L., Flocke, F., Lueb, R. A., Stroud, V., and Travnicek, W.:
28 Measurements of bromine containing organic compounds at the tropical tropopause, *Geophys.*
29 *Res. Lett.*, 25, 317-320, 10.1029/98GL00040, 1998.
- 30 Schlundt, M., Brandt, P., Dengler, M., Hummels, R., Fischer, T., Bumke, K., Krahnemann, G.,
31 and Karstensen, J.: Mixed layer heat and salinity budgets during the onset of the 2011
32 Atlantic cold tongue, *J. Geophys. Res.-Oceans*, 119, 7882-7910, 10.1002/2014jc010021,
33 2014.
- 34 Smythe-Wright, D., Boswell, S. M., Breithaupt, P., Davidson, R. D., Dimmer, C. H., and
35 Diaz, L. B. E.: Methyl iodide production in the ocean: Implications for climate change, *Glob.*
36 *Biogeochem. Cycles*, 20, Gb3003, 10.1029/2005gb002642, 2006.
- 37 Smythe-Wright, D., Peckett, C., Boswell, S., and Harrison, R.: Controls on the production of
38 organohalogens by phytoplankton: Effect of nitrate concentration and grazing, *J. Geophys.*
39 *Res.-Biogeosci.*, 115, 10.1029/2009jg001036, 2010.
- 40 Solomon, S., Garcia, R. R., and Ravishankara, A. R.: On the role of iodine in ozone depletion,
41 *J. Geophys. Res.-Atmos.*, 99, 20491-20499, 10.1029/94jd02028, 1994.
- 42 Stramma, L., and Schott, F.: The mean flow field of the tropical atlantic ocean, *Deep-Sea Res.*
43 *Part II-Top. Stud. Oceanogr.*, 46, 279-303, 10.1016/s0967-0645(98)00109-x, 1999.

- 1 Taylor, B. B., Torrecilla, E., Bernhardt, A., Taylor, M. H., Peeken, I., Rottgers, R., Piera, J.,
2 and Bracher, A.: Bio-optical provinces in the eastern atlantic ocean and their biogeographical
3 relevance, *Biogeosciences*, 8, 3609-3629, 10.5194/bg-8-3609-2011, 2011.
- 4 Tegtmeier, S., Krüger, K., Quack, B., Atlas, E. L., Pisso, I., Stohl, A., and Yang, X.: Emission
5 and transport of bromocarbons: From the west pacific ocean into the stratosphere, *Atmos.*
6 *Chem. Phys.*, 12, 10633-10648, 10.5194/acp-12-10633-2012, 2012.
- 7 Tegtmeier, S., Krüger, K., Quack, B., Atlas, E., Blake, D. R., Boenisch, H., Engel, A.,
8 Hepach, H., Hossaini, R., Navarro, M. A., Raimund, S., Sala, S., Shi, Q., and Ziska, F.: The
9 contribution of oceanic methyl iodide to stratospheric iodine, *Atmos. Chem. Phys.*, 13, 11869-
10 11886, 10.5194/acp-13-11869-2013, 2013.
- 11 Tokarczyk, R., and Moore, R. M.: Production of volatile organohalogenes by phytoplankton
12 cultures, *Geophys. Res. Lett.*, 21, 285-288, 10.1029/94GL00009, 1994.
- 13 Tomczak, M., and Godfrey, J. S.: *Regional oceanography: An introduction*, in, 2 ed., Daya
14 Publishing House, Delhi, 2005.
- 15 Tsuchiya, M., Talley, L. D., and McCartney, M. S.: An eastern atlantic section from iceland
16 southward across the equator, *Deep-Sea Res.*, 39, 1885-1917, 10.1016/0198-0149(92)90004-
17 d, 1992.
- 18 Veldhuis, M. J. W., and Kraay, G. W.: Phytoplankton in the subtropical atlantic ocean:
19 Towards a better assessment of biomass and composition, *Deep-Sea Res. Part I-Oceanogr.*
20 *Res. Pap.*, 51, 507-530, 10.1016/j.dsr.2003.12.002, 2004.
- 21 Wang, L., Moore, R. M., and Cullen, J. J.: Methyl iodide in the nw atlantic: Spatial and
22 seasonal variation, *J. Geophys. Res.-Oceans*, 114, C07007, 10.1029/2007jc004626, 2009.
- 23 Weingartner, T. J., and Weisberg, R. H.: On the annual cycle of equatorial upwelling in the
24 central aatlantic-ocean, *J. Phys. Oceanogr.*, 21, 68-82, 10.1175/1520-
25 0485(1991)021<0068:otacoe>2.0.co;2, 1991.
- 26 Yamamoto, H., Yokouchi, Y., Otsuki, A., and Itoh, H.: Depth profiles of volatile halogenated
27 hydrocarbons in seawater in the bay of bengal, *Chemosphere*, 45, 371-377, 10.1016/s0045-
28 6535(00)00541-5, 2001.
- 29 Zika, R. G., Gidel, L. T., and Davis, D. D.: A comparison of photolysis and substitution
30 decomposition rates of methyl-iodide in the ocean, *Geophys. Res. Lett.*, 11, 353-356,
31 10.1029/GL011i004p00353, 1984.
- 32 Ziska, F., Quack, B., Abrahamsson, K., Archer, S. D., Atlas, E., Bell, T., Butler, J. H.,
33 Carpenter, L. J., Jones, C. E., Harris, N. R. P., Hepach, H., Heumann, K. G., Hughes, C.,
34 Kuss, J., Krüger, K., Liss, P., Moore, R. M., Orlikowska, A., Raimund, S., Reeves, C. E.,
35 Reifenhäuser, W., Robinson, A. D., Schall, C., Tanhua, T., Tegtmeier, S., Turner, S., Wang,
36 L., Wallace, D., Williams, J., Yamamoto, H., Yvon-Lewis, S., and Yokouchi, Y.: Global sea-
37 to-air flux climatology for bromoform, dibromomethane and methyl iodide, *Atmos. Chem.*
38 *Phys.*, 13, 8915-8934, 10.5194/acp-13-8915-2013, 2013.